International Journal of Pharmaceutics 662 (2024) 124529

Contents lists available at ScienceDirect

International Journal of Pharmaceutics

journal homepage: www.elsevier.com/locate/ijpharm

Cancer cell membrane-modified Soluplus® micelles for gemcitabine delivery to pancreatic cancer using a prodrug approach

Miguel Pereira-Silva [a,b,c], Luis Diaz-Gomez [c], Bárbara Blanco-Fernandez [c], Alba Ferreirós [d], Francisco Veiga [a,b], Angel Concheiro [c], Ana Cláudia Paiva-Santos [a,b], Carmen Alvarez-Lorenzo [c,*]

[a] Department of Pharmaceutical Technology, Faculty of Pharmacy of the University of Coimbra, University of Coimbra, 3000-548 Coimbra, Portugal
[b] REQUIMTE/LAQV, Group of Pharmaceutical Technology, Faculty of Pharmacy of the University of Coimbra, University of Coimbra, 3000-548 Coimbra, Portugal
[c] Departamento de Farmacología, Farmacia y Tecnología Farmacéutica, I+D Farma (GI-1645), Faculty of Pharmacy, Institute of Materials (iMATUS), and Health Research Institute of Santiago de Compostela (IDIS), Universidade de Santiago de Compostela, 15782 Santiago de Compostela, Spain
[d] Nasasbiotech, S.L., Canton Grande 9, 15003 A Coruña, Spain

ARTICLE INFO

Keywords:
Polymeric micelle
Soluplus®
Pancreatic cancer
Gemcitabine
Prodrug delivery
Cancer cell membrane modification

ABSTRACT

Pancreatic cancer (PC) is one of the most lethal malignancies worldwide and its incidence is increasing. Chemotherapy is often associated to limited efficacy, poor targeting and systemic toxicity. In this work, the hydrophilic gemcitabine (GEM), widely used in PC treatment alone or in combination, was conjugated with vitamin E succinate (VES) and encapsulated in Soluplus® micelles. This prodrug approach facilitated encapsulation of the anticancer drug into the self-assembled copolymer micelles. Soluplus®/VES-GEM micelles were optimized regarding the ratio of the components and the preparation process. The micelles were small-sized (<80 nm), monodisperse, and highly stable, efficiently retaining the conjugate drug and showing significant antiproliferative activity against BxPC3 cell line. To improve biofunctionalization and targeting properties of prepared Soluplus®/VES-GEM micelles, biomimetic modification with PC cell membrane was further attempted by co-extruding PC cell membrane (BxPC3) nanovesicles with Soluplus®/VES-GEM micelles. Several protocols were attempted to prepare the BxPC3-modified Soluplus®/VES-GEM micelles and the outcomes were analyzed in detail. Overall, the results pave the way to innovative PC-targeted nanotherapies by maximizing GEM encapsulation in hydrophobic compartments with high stability and affinity. The results also highlight the need of higher resolution techniques to characterize cell membrane coating of nanocarriers bearing highly hydrophilic shells.

1. Introduction

Pancreatic cancer is a hard-to-treat cancer subtype with an average 5-year survival rate of 3 % (Siegel et al., 2024). Although conventional chemotherapy remains a key treatment, its effectiveness has not significantly improved in the last 30 years due to impaired pharmacokinetics and systemic toxicity (Mao et al., 2024). Hence, new drug delivery strategies are needed to improve the efficacy and safety of the treatments. Nanosystems, tailored to the nanoscale, offer unique properties such as increased surface area, enhanced biointerface, and improved stability and blood circulation of drugs, while minimizing adverse effects. Several nanosystems, including liposomes, micelles and nanoparticles, are being tested for pancreatic cancer therapy (Raza et al., 2023; Tarannum and Vivero-Escoto, 2022; Pramanik et al., 2024).

In recent years, amphiphilic copolymers have been explored as versatile units for improved drug pharmacokinetics as building blocks for polymeric micelles (Ghosh and Biswas, 2021; Quan et al., 2014). The hydrophobic core of polymeric micelles is particularly suitable for hosting hydrophobic drugs, while the stealth hydrophilic shell, often composed of polyethylene glycol (PEG), can extend blood circulation and minimize immune uptake (Zhang et al., 2022). Polyvinyl caprolactam–polyvinyl acetate–polyethylene glycol graft copolymer, PEG-g-(PVAc-co-PVCL), with composition of 13 % PEG 6000/57 % vinyl caprolactam/30 % vinyl acetate, also known as Soluplus®, is a biocompatible non-ionic amphiphilic polymer used mainly for oral solubilization, with molecular weight of 90,000–140,000 g/mol (Attia

* Corresponding author.
E-mail address: carmen.alvarez.lorenzo@usc.es (C. Alvarez-Lorenzo).

https://doi.org/10.1016/j.ijpharm.2024.124529
Received 14 June 2024; Received in revised form 25 July 2024; Accepted 25 July 2024
Available online 30 July 2024

et al., 2023). Soluplus® enhances bioavailability of hydrophobic drugs (Zeng et al., 2017; Zhou et al., 2022) acting as an absorption enhancer (Attia et al., 2023; Basha et al., 2020; Alopaeus et al., 2019). Moreover, Soluplus® shows multidrug resistance reversal (MDR) properties, *via* P-glycoprotein (P-gp) inhibition (Zeng et al., 2017), a key transporter in drug resistance (Pote and Gacche, 2023).

Soluplus® self-assembles into micelles with high colloidal stability and low critical micellar concentration (CMC) (8×10^{-3} mg/mL), resulting in an attractive excipient for micelle-based formulations (Dian et al., 2014; Riedel et al., 2022). The low CMC and compact structure of Soluplus® micelles provides stability in serum, improving the *in vivo* stability and preventing disintegration in blood (Alambiaga-Caravaca et al., 2020; Twal et al., 2024). Soluplus®-based micelles have shown improved tumor bioavailability and antitumoral properties, benefiting from the stealth properties of PEG substitution and the solubilization capacity of the hydrophobic core (Wang et al., 2020; Jin et al., 2015). They have been tested for delivering anticancer drugs, such as doxorubicin (Jin et al., 2020), lapatinib (Bonde et al., 2020), and *posidonia oceanica* extract (Piazzini et al., 2019). Additionally, Soluplus® has been explored in mixed copolymer systems with other co-surfactants, such as Pluronic® F127 (Dian et al., 2014; Singh et al., 2018), Pluronic® F68 (Dong et al., 2023), chitosan (Twal et al., 2024), and TPGS (Riedel et al., 2022; Ding et al., 2020; Feng et al., 2020; Wang et al., 2019; Zhao et al., 2017) for targeted chemotherapy and other therapeutic applications (Bernabeu et al., 2016; Jiang et al., 2019).

The anti-metabolite deoxycytidine analogue gemcitabine (GEM) is extensively used in pancreatic cancer chemotherapy, either alone or with albumin-bound paclitaxel (Abraxane®). GEM triphosphate, the active form of GEM, is produced through phosphorylation and inhibits DNA synthesis by incorporating into DNA. However, intravenous GEM administration faces challenges like off-target toxicity, poor cell internalization, high susceptibility to enzymatic degradation and fast clearance from the body. By modifying GEM with lipidic moieties, a prodrug system can respond to physiological cues such as enzymes (e.g., Cathepsin B) (Han et al., 2022; Jeon et al., 2022; Li et al., 2020; Wu et al., 2020). Therefore, the combination of nanosystems with a prodrug approach is an attractive strategy for leveraging pancreatic cancer-targeted therapeutics.

Despite significant advancements in nanosystem-based drug delivery, their tumor-targeting efficiency remains low (~0.7 %, with only 0.8 % in pancreatic cancer), highlighting a major bottleneck in cancer therapeutics (Jeon et al., 2022). Recently, biomimetic nanosystems have emerged as versatile platforms mimicking physiological structures and processes to enhance biocompatibility, biointerfacing and targeting features (Wilhelm et al., 2016). Cell membrane-coated nanosystems combine the functional attributes of native cell membranes with the versatility of nanoparticle cores by enveloping cores with extracted cell membranes of distinct origin through a simple co-extrusion approach. Particularly cancer cell membrane-coated nanosystems offer enhanced homotypic targeting, immune escape, and prolonged blood circulation of nanoparticle cores by a camouflaging mechanism mediated by the biocompatible lipidic bilayer expressing CD-47 "self'-markers (Pan et al., 2024; Lu et al., 2024; Pereira-Silva et al., 2020). Several studies have reported improved pharmacokinetic properties with micelle cores coated with membranes from red blood cells (Malhotra et al., 2021), cancer cells (Pereira-Silva et al., 2020; Jin et al., 2024), macrophages (Zhang et al., 2024) and hybrid sources (Huang et al., 2024).

The aim of this work was to prepare GEM-loaded Soluplus® micelles (Soluplus®/VES-GEM) for intracellular GEM delivery and enhanced synergistic PDAC therapy. This all-functional nanosystem combines vitamin E succinate (VES) (Fig. 1. **A**) coupled to GEM (Fig. 1. **B**) (Fang et al., 2015; Pereira-Silva et al., 2024) and loaded into Soluplus® (Fig. 1. **C**) micelles. This approach represents, to the best of our knowledge, the first micelle nanosystem incorporating both Soluplus® and a prodrug conjugate as amphiphilic micelle unit. The innovative PC cell membrane coating strategy aims to improve biointerfacing features and stands as one of the first applications of cell membrane-modified micelle systems in PC therapy.

Specifically, Soluplus®/VES-GEM formulation was explored to 1) enable GEM encapsulation in a micelle system, 2) improve solubility of VES-GEM, 3) confer improved stability, protection and ultra-sustained release profile to GEM and VES-GEM, 4) show significant cytotoxic activity against PC cells (BxPC3 cell line), further providing 5) insights regarding possibility of coating a Soluplus®-based micelle system with PC cell membrane and elucidation of combined action of the obtained PC membrane-obtained formulation on improving cytotoxic activity of the GEM-loaded prodrug. Soluplus®/VES-GEM micelles were prepared *via* solvent evaporation method, at distinct mole ratios, and characterized regarding size, surface charge (zeta potential) and polydispersity index, encapsulation efficiency and drug loading. *In vitro* assays were conducted to elucidate the therapeutic potential of Soluplus®/VES-GEM micelles regarding cytotoxicity, internalization, and haemolytic activity. Finally, the feasibility of a coating based on PC cell membrane was explored.

2. Materials and methods

2.1. Materials

Gemcitabine hydrochloride (GEM·HCl, $C_9H_{11}F_2N_3O_4$·HCl) (MW 299.66 g/mol), Triton-X-100, poly(lactic-co-glycolic acid) nanoparticles (PLGA, 0.67 dL/g carboxy-terminated 50:50, MW 24,000–38,000), bovine serum albumin (BSA), 1,2-dioleoyl-*sn*-glycero-3-phosphoethanolamine labelled with Atto 488 (DOPE-Atto 488) and RPMI-1640

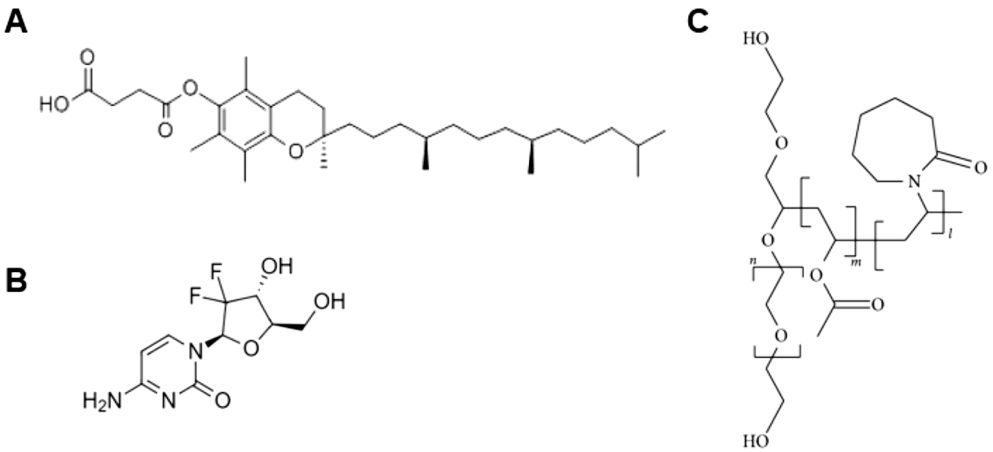

Fig. 1. Chemical structures of vitamin E succinate (A), gemcitabine (B) and Soluplus® (C).

medium supplemented with 10 % of FBS and 1 % antibiotics were purchased from Sigma-Aldrich (St. Louis, MO, USA). Vitamin E succinate (VES) (MW 530.80 g/mol) was purchased from Santa Cruz Biotechnology Inc. (Dallas, TX, USA); Soluplus® (polyvinyl caprolactam-polyvinyl acetate-polyethylene glycol copolymer) (MW ~ 115,000 g/mol) was purchased from BASF® (Ludwigshafen, Germany); sodium 1-heptanesulfonate (MW 220.26 g/mol) was purchased from Fluka Chemie (Buchs, Switzerland); di-sodium hydrogen phosphate dihydrate ($Na_2HPO_4{\cdot}2H_2O$); ethanol absolute with purity > 99.9 %, methanol (HPLC grade) and sodium hydroxide (NaOH) were purchased from VWR Chemicals (Leuven, Belgium); sodium dihydrogen phosphate anhydrous AGR (NaH_2PO_4) and sodium chloride (NaCl) were purchased from Labkem (Barcelona, Spain); potassium chloride (KCl) and potassium di-hydrogen phosphate (KH_2PO_4) were from Panreac AppliChem (Barcelona, Spain). Ultrapure water was continuously obtained from Milli-Q® Benchtop Lab Water Purification System (Millipore Ibérica, Madrid, Spain). Hydrophilic polytetrafluoroethylene (PTFE) syringe filters (13 mm, 0.2 μm; 25 mm, 0.4 μm), tris hydrochloride (Tris-HCl) and magnesium chloride ($MgCl_2$) were purchased from Scharlab S.L. (Barcelona, Spain). EDTA-free Pierce Protease Inhibitor Tablets were obtained from Thermo Fisher, (Madrid, Spain). 4′,6-Diamidino-2-phenylindole (DAPI), Nile red and 1,1′-dioctadecyl-3,3,3′,3′-tetramethylindodicarbocyanine (DiD) were purchased from Invitrogen™, Thermo Fisher (Madrid, Spain). Nylon membrane discs (47 mm, 0.2 μm) were obtained from Pall Corporation (Waters, Ann Arbor, MI, USA). Phosphate buffered saline (PBS, 0.01 M, pH = 7.4) was prepared with 8 g/L NaCl, 0.2 g/L KCl, 1.44 g/L $Na_2HPO_4{\cdot}2H_2O$, and 0.24 g/L KH_2PO_4. All additional reagents were of analytical or HPLC grade and used following the manufacturer's instructions.

2.2. HPLC quantification methods

A RP-HPLC system JASCO (AS-4150 RHPLC Autosampler, PU-4180 RHPLC Pump, LC-NetII/ADC Interface Box, CO-4060 Column Oven, MD-4010 Photo Diode Array Detector) was used. For the quantification of VES-GEM conjugate, a Zorbax Eclipse XDB-C18 column (5 μm, 4.6 mm × 250 mm) at 30 °C and methanol as mobile phase, flow rate 1 mL/min, was used. Detection wavelength was set at 248 nm (Fang et al., 2015). GEM content was quantified using a Waters Spherisorb ODS2 column (5 μm, 4.6 mm × 250 mm) at 40 °C and a mixture of buffer and acetonitrile (90:10) as mobile phase, flow rate 1 mL/min (Kirstein et al., 2006). The detection wavelength was set at 268 nm. The buffer solution was composed of sodium dihydrogen phosphate anhydrous (6 g/L) and 1-heptanosulfonate as ion pairing reagent (0.660 g/L), pH 3, corrected with triethylamine and orthophosphoric acid. The buffer solution was filtered through nylon membrane disc (47 mm, 0.2 μm), Pall corporation (MI, USA). All samples were filtered before injection through PTFE hydrophilic syringe filter (13 mm, 0.22 μm), Scharlab S.L. (Barcelona, Spain). Injection volume was 20 μL.

2.3. Soluplus®/VES-GEM micelles preparation

First, solutions of VES-GEM conjugate (6 mg) in ethanol (5 mL) were prepared in parallel under stirring (400 rpm) at room temperature (RT) for 4 h, protected from light (final concentration 1.2 mg/mL VES-GEM in ethanol). Then, different amounts of Soluplus® (120 mg, 256 mg) were individually added to the ethanolic VES-GEM solution followed by stirring (400 rpm) at RT for 3 h. The obtained mixture composed of Soluplus® and VES-GEM conjugate in ethanol was added dropwise (1 drop/s) to either PBS diluted in MiliQ® water (50:50 *v/v*, 15 mL) or NaCl 0.45 % *w/v* in MiliQ® water, under agitation (300 rpm) and kept under gentle magnetic stirring (250 rpm), protected from light at RT overnight and open in a biological safety cabinet to ensure ethanol evaporation (**Figure S1**).

Different Soluplus®/VES-GEM mole ratios were obtained (0.14/1 and 0.30/1) by fixing VES-GEM concentration (0.4 mg/mL) and varying Soluplus® concentration. Next, a set of Soluplus®/VES-GEM formulations with mole ratios 0.25/1, 0.50/1, 1.0/1 and 1.50/1 (Table 1) was prepared to explore the effect of Soluplus® concentrations on VES-GEM solubilization, following the same procedure. For decreasing VES-GEM concentration, a set of Soluplus®/VES-GEM 0.75/1 mole ratio micelles (29.8 mg/mL Soluplus®, 0.267 mg/mL VES-GEM) were prepared as described in PBS diluted in MiliQ® water (50:50 *v/v*) (**Table S1**). Different batches were prepared for assessing batch-to-batch variation.

Blank Soluplus® micelles were prepared by dissolving Soluplus® in PBS diluted in MiliQ® water (50:50 *v/v*), under stirring (300 rpm) at RT for 3 h. Poly(lactic-co-glycolic acid) (PLGA) nanoparticles were prepared by solvent evaporation method. Briefly, PLGA (0.67 dL/g carboxy-terminated 50:50 PLGA, 5 mg) was dissolved in acetone (5 mL) and the mixture added dropwise to 5 mL MiliQ® water under stirring at 300 rpm and left overnight for acetone evaporation. Final concentration of PLGA was 1 mg/mL.

2.4. Effect of VES-GEM conjugate on Soluplus® micellization

The effect of VES-GEM on the self-assembly of Soluplus® micelles was evaluated using a surface tension assay, employing the *Du Noüy* Ring method (Holland et al., 2023; Ch et al., 2023). In brief, a set of Soluplus® dispersions in PBS: water 50:50 *v/v* were prepared in varying concentrations (5×10^{-3}, 1×10^{-2}, 5×10^{-2}, 0.1, 0.3, 0.5, 1 mg/mL) and the dispersions were added to Eppendorf vials (9.90 mL). In parallel, a stock solution of VES-GEM in ethanol (500 μL, 1.35×10^{-1} mg/mL) was prepared and aliquots (100 μL) were added to Eppendorf vials containing the Soluplus® dispersions, to achieve final volume of 10 mL. Blank Soluplus® micelles were prepared as described above (Mateos et al., 2022). All formulations were left overnight in a hood without stirring, protected from light at RT, to allow ethanol evaporation. The surface tension for each solution was recorded the next day using a Platinum ring in a tensiometer TD 1 Lauda (Fisher Scientific Hucoa, Madrid, Spain) (Liu et al., 2022).

2.5. Soluplus®/VES-GEM micelles characterization

2.5.1. Micelle size, PDI and zeta potential

Micelle size distribution, polydispersity index (PDI) and zeta potential (ZP) of the different formulations were measured by dynamic light scattering (DLS) at 25 °C with a scattering angle of 173° (Zetasizer Nano ZS, Malvern Instruments SA, UK) (Emamzadeh et al., 2018). To test the effect of filtration on the size, PDI and ZP of the formulations, the formulations were tested in parallel before and after filtration through 0.4

Table 1
Size, zeta potential and polydispersity index of Soluplus®/VES-GEM micelles, prepared in PBS:water (50:50 *v/v*) media, mole ratio (0.25/1, 0.5/1, 1/1 and 1.5/1) and in the presence or absence of filtration. VES-GEM mass fixed 6 mg/vial (0.4 mg/mL final concentration).

SOLUPLUS®/VES-GEM	pH	Size (nm) ± S.D.	ZP (mV) ± S.D.	PDI±S.D.
1.5/1 with filter	6.31	127.5 ± 0.9	0.111 ± 0.190	0.194 ± 0.003
1.5/1 without filter		205.0 ± 11.5	0.690 ± 0.965	0.444 ± 0.020
1/1 with filter	6.83	111.6 ± 19.4	−0.300 ± 0.497	0.212 ± 0.023
1/1 without filter		465.3 ± 151.3	0.212 ± 0.435	0.595 ± 0.132
0.5/1 with filter	7.41	87.7 ± 0.2	−0.903 ± 0.985	0.030 ± 0.010
0.5/1 without filter		352.3 ± 71.2	−1.152 ± 0.225	0.486 ± 0.062
0.25/1 with filter	7.31	99.1 ± 0.9	−1.335 ± 0.373	0.191 ± 0.019
0.25/1 without filter		304.7 ± 25.9	−1.406 ± 0.265	0.364 ± 0.035

nm PTFE filter (n = 3).

2.5.2. Encapsulation efficiency and drug loading

The concentrations of GEM and VES-GEM conjugate in the formulations were determined by RP-HPLC (Fang et al., 2015; Khare et al., 2016). For GEM quantification present in the conjugate, a prior alkaline hydrolysis with 0.1 M NaOH (1 h/40 °C) was performed to release GEM from the VES-GEM conjugate to enable free drug quantification. Encapsulation efficiency (EE%) was calculated as the ratio of the quantified amount of GEM and the initially weighed amount of GEM added to the mixture, expressed as percentage (**equation (1)**.

$$EE\,(\%) = \frac{Quantified\ \ amount\ \ of\ \ GEM\ \ in\ \ micelles\ \ (mg)}{Theoretical\ \ amount\ \ of\ \ GEM\ \ in\ \ micelles\ \ (mg)} \times 100 \quad (1)$$

Drug loading (DL%) was calculated as the quotient between the amount of quantified GEM *versus* the weighed amount of VES-GEM and Soluplus® used to prepare the micelles, expressed as percentage (**equation (2)**.

$$DL\,(\%) = \frac{Quantified\ \ amount\ \ of\ \ GEM\ \ in\ \ the\ \ micelles\ \ (mg)}{\begin{array}{c}Weighed\ \ amount\ \ of\ \ VES-GEM+\\ Soluplus®\ \ in\ \ the\ \ micelles\ \ (mg)\end{array}} \times 100 \quad (2)$$

For VES-GEM conjugate quantification, aliquots of micelle formulation (100 µL) were diluted in ethanol (1:9 *v/v*) to allow disruption of micelle structure, vortexed 2 s (Reax top model, Heidolph Instruments GmbH & Co. KG, Schwabach, Germany), filtered using PTFE hydrophilic Scharlau syringe filter (13 mm, 0.22 µm), followed by HPLC quantification. EE (%) was calculated as the quotient between quantified amount of VES-GEM and initial weighed amount of VES-GEM added to the mixture (**equation (3)**, and DL (%) as the quotient between amount of quantified VES-GEM and weighed amount of VES-GEM and Soluplus® used to prepare the micelles (**equation (4)**.

$$EE\,(\%) = \frac{\begin{array}{c}Quantified\ \ amount\ \ of\ \ VES-GEM\ \ conjugates\\ in\ \ the\ \ micelles\ \ (mg)\end{array}}{\begin{array}{c}Weighed\ \ amount\ \ of\ \ VES-GEM\ \ conjugates\\ in\ \ the\ \ micelles\ \ (mg)\end{array}} \times 100 \quad (3)$$

$$DL\,(\%) = \frac{\begin{array}{c}Quantified\ \ amount\ \ of\ \ VES-GEM\ \ conjugates\\ in\ \ the\ \ micelles\ \ (mg)\end{array}}{\begin{array}{c}Weighed\ \ amount\ \ of\ \ VES-GEM\ \ conjugates+\\ Soluplus®\ \ in\ \ the\ \ micelles\ \ (mg)\end{array}} \times 100 \quad (4)$$

Purification of Soluplus®/VES-GEM micelles by filtration was carried out using hydrophilic PTFE syringe filter (25 mm, 0.4 µm), and aliquots were collected and diluted in ethanol 1:9 *v/v*, as previously described. EE (%) was calculated according to **equation (3).** Purification by centrifugation was carried out by centrifugation (centrifuge model 5804R, Eppendorf AG, Hamburg, Germany) in two parallel settings: centrifugation at 12,000 rpm, 20 min, at 4 °C, and centrifugation at 4000 rpm, 30 min, at 4 °C (Alambiaga-Caravaca et al., 2020; Grimaudo et al., 2018). Aliquots were then collected, diluted in ethanol 1:4 *v/v* and analysed through HPLC, as described before. EE (%) was calculated following **equation (3).** Purification through ultrafiltration was performed using Amicon Ultra 0.5 mL Centrifugal filters, 100 kDa (Merck Millipore, Ireland) at 1000 rpm, 3 min, at 25 °C (Rouco et al., 2022). The subnatant was collected in triplicates and diluted 1:4 *v/v* in ethanol, and VES-GEM concentration was quantified through HPLC, and the EE (%) was calculated (**equation (3)**.

2.5.3. Morphology

The morphology of the micelles was evaluated using two different methods: phosphotungstic acid and uranyl acetate staining. For phosphotungstic acid staining, formulations were negatively stained with 2 % phosphotungstic acid for 2 min and observed on a TEM JEM1011 at 80 kV (JEOL, Peabody, MA, USA). For uranyl acetate dyeing, formulations (20 µL) were placed on carbon-copper grids. Then, 20 µL of uranyl acetate 2 % (*w/v*) were added to the formulation and, after 5 min, and the grids were washed thrice with MiliQ® water (0.1 mL) and the excess was drained with filter paper. The stained formulations were dried overnight in a hood and protected from light and further observed by TEM and FESEM (GeminiSEM, GEMINI 500, Zeiss, Oberkocken, Germany) at 20 kV.

2.5.4. Soluplus®/VES-GEM micelles absorbance spectra

The UV–Vis spectra of VES-GEM conjugate in ethanol (0.267 mg/mL), Soluplus® micelles at 29.8 mg/mL without and with VES-GEM conjugate (0.267 mg/mL) in PBS:water 50:50 *v/v*, as well as diluted 1:9 *v/v* counterparts (VES-GEM diluted with ethanol and the remaining ones in PBS:water 50:50 *v/v*) were recorded in the 190–800 nm range using a UV–Vis spectrophotometer (Agilent 8534, Waldbronn, Germany). Sampling points were taken every 1 nm using a quartz cell of 10 mm light path. Ethanol and PBS (50:50) were used as blanks for VES-GEM conjugate and Soluplus® micelles, respectively.

2.6. Saturation solubility studies

VES-GEM solubility study was performed by adding increasing concentrations of solution of VES-GEM in ethanol (0.8 mg/mL) to aqueous Soluplus® dispersions (50:50 *v/v* PBS:water, 1 mL) with fixed polymer concentration (29.8 mg/mL) under 300 rpm stirring overnight at RT, protected from light and in a hood to allow ethanol evaporation (**Table S2**).

The next day, the dispersions were centrifuged at 4000*g* for 30 min at 4 °C using a centrifuge 5804R (Eppendorf AG, Hamburg, Germany) to separate non-solubilized VES-GEM. The supernatants were collected and diluted 1:4 *v:v* in ethanol for VES-GEM quantification through HPLC to determine the apparent solubility of VES-GEM (Varela-Garcia et al., 2018; Vivero-Lopez et al., 2022). As control, the VES-GEM ethanolic solution was added to 50:50 *v/v* PBS:water medium.

2.7. VES-GEM conjugate release profile

The release of VES-GEM conjugate from Soluplus®/VES-GEM micelles was performed using dialysis at pH 7.4 and pH 5 (n = 3) (Pereira-Silva et al., 2024). Briefly, 1 mL aliquots of Soluplus®/VES-GEM micelles were placed inside dialysis membrane bags with MWCO of 12.4 kDa (D9652-100FT, Sigma-Aldrich, St. Louis, MO, USA). The bags were sealed and placed in beakers containing 0.5 % Tween 80® in PBS (15 mL) pH 7.4 and pH 5, and incubated at 100 rpm/37 °C in a shaker (Incubator 1000, Heidolph Instruments GmbH & Co. KG, Schwabach, Germany) during 1 week, protected from light. Samples of the release medium (0.25 mL) were collected at predetermined time points (0.5, 1, 2, 4, 8, 12, 24, 48, 72, and 168 h) for VES-GEM quantification. The collected aliquots were diluted 1:1 *v/v* in ethanol, vortexed for 2 s, and filtered through a 0.22 µm membrane filter before HPLC analysis. The dialysis membrane was pre-wetted according to the manufacturer (Xu et al., 2015). The experiment was further performed using distinct parameters, including variations in the release medium, release medium volume, solubilizer agent, and dialysis bag apparatus, to facilitate VES-GEM release (Table 2).

Other variables investigated were: vortexing of release medium before sampling, vortexing of collected aliquots in Eppendorf vials before ethanol dilution, vortexing time for the collected aliquots in ethanol, ethanol dilution proportion (1:1, 1:2, 1:4, 1:9 *v/v* aliquot: ethanol), solvent (ethanol, methanol, acetonitrile, dimethyl sulfoxide (DMSO), water, no dilution) and the section of filtered diluted aliquots placed inside the HPLC vials with inserts (to evaluate filter clogging, heterogeneous distribution of VES-GEM and formation of precipitates). The VES-GEM content inside the bags was also quantified through HPLC. Briefly, bags were open, and aliquots were collected in duplicates at opposite sites, diluted in ethanol 1:4 *v/v* and previous procedure was

Table 2
Variables evaluated during the VES-GEM release tests from Soluplus®/VES-GEM micelles (0.75/1) prepared in PBS:water (50:50 *v/v*) medium, and VES-GEM content quantified in the release medium after 72 h of incubation. The volume of formulation inside the bag was 1 mL.

Release medium	Release medium volume (mL)	Solubilizer	Dialysis bag setting	VES-GEM analysis (HPLC)
PBS pH 7.4	15	None	Cylindrical	< LOQ
PBS pH 7.4	50	Tween 80® (0.5 %v/v)	Cylindrical	< LOQ
PBS pH 7.4	15	Tween 80® (0.5 %v/v)	Flat	< LOQ
PBS pH 7.4	15	Tween 80® (1.0 %v/v)	Cylindrical	< LOQ
PBS pH 7.4	15	Albumin (5 % v/v)	Cylindrical	< LOQ
PBS pH 7.4	15	PEG2000 (1 % v/v)	Cylindrical	< LOQ
PBS pH 7.4	15	SDS (1 % v/v)	Cylindrical	< LOQ
PBS pH 7.4	15	DMSO (1 % v/v)	Cylindrical	< LOQ
PBS pH 7.4	15	Soluplus® (3 % v/v)	Cylindrical	< LOQ
PBS pH 7.4	15	TPGS (1 % v/v)	Cylindrical	>LOQ, peak interference
Culture medium	15	None	Cylindrical	< LOQ
PBS pH 7.4: EtOH 80:20 v/v	15	EtOH (20 % v/v)	Cylindrical	< LOQ

followed. For assessing sink conditions, an excess of powdered VES-GEM (2 mg) was added to Eppendorf vials (1 mL, Tween 80® 0.5 % in PBS pH 7.4), left stirring 48 h at 350 rpm, protected from light, and filtered through 0.22 μm membrane filter, diluted in ethanol 1:9 *v/v*, and quantified by HPLC as described in section 2.5.

2.8. Stability of Soluplus®/VES-GEM micelles

2.8.1. Stability in PBS

Soluplus®/VES-GEM micelles prepared in PBS:water 50:50 *v/v* were incubated either at 4 °C without stirring or at 37 °C in a shaker under gentle stirring (100 rpm), for 4 weeks and light protected (Wang et al., 2014). Samples were collected at predetermined time points, GEM and VES-GEM content was monitored through HPLC, and micelle size, ZP and PDI were evaluated through DLS.

2.8.2. Stability upon dilution

Stability upon dilution of Soluplus®/VES-GEM micelles (prepared with 29.8 mg/mL Soluplus®) was tested by diluting 1000 times the formulations with and without VES-GEM in PBS:water 50:50 *v/v*. The diluted samples were maintained at RT for 1 h without stirring before DLS measurement to assess changes in size, ZP and PDI (Grimaudo et al., 2018; Vivero-Lopez et al., 2022).

2.8.3. Stability in protein medium

Soluplus® micelles (29.8 mg/mL, 0.1 mL) were incubated with BSA (8 mg/mL, 0.9 mL), 1:9 *v/v*, and the mixture was incubated for 24 h at RT under gentle stirring (100 rpm) (He et al., 2023; Luo et al., 2022). Aliquots were collected at predetermined time points (0 h, 1 h, 8 h and 24 h) and the size, ZP, and PDI were obtained.

2.8.4. Batch-to-batch variation

A set of Soluplus®/VES-GEM micelles (29.8 mg/mL Soluplus® and 0.267 mg/mL VES-GEM, 3.75 mL) prepared on different days, as described before, were characterized regarding size and PDI to assess the extension of batch-to-batch variation. The formulations were not filtered and were analysed maximum 24 h after preparation and were kept stirring (200 rpm) at RT before measurement.

2.9. Blood compatibility

The blood compatibility of Soluplus®/VES-GEM micelles was assessed according to a previous protocol (Pereira-Silva et al., 2024). Briefly, human blood obtained from anonymized healthy donors, under written informed consent and according to Spanish legislation (Law 14/2007 on Biomedical Research), was diluted in PBS (3.5 % *v/v*). Blank Soluplus® and Soluplus®/VES-GEM micelles (0.1 mL) were added to diluted blood (0.9 mL), and the mixture was incubated at 37 °C for 1 h at 100 rpm. Then, the samples were centrifuged at 2655*g* for 10 min, the supernatants were collected, and the absorbance of released haemoglobin from lysed erythrocytes was read at 540 nm in a plate reader (FLUOstar optima, BMG LabTech, Ortenberg, Germany). Hemolysis was calculated as the extent of hemolytic activity according to Equation (5):

$$Hemolysis(\%) = \frac{A_S - A_N}{A_P - A_N} \times 100 \quad (5)$$

A_S represents sample absorbance, A_N stands for the absorbance of the negative control (blood diluted in PBS), and A_P is the absorbance of the positive control (diluted blood mixed with Triton X-100 1 % *v/v*).

2.10. Cell viability in 2D model

Human pancreatic cancer BxPC3 cells (ATCC CRL-1687™, ATCC, USA) were cultured in RPMI-1640 medium supplemented with 10 % of FBS and 1 % antibiotics (10,000 U/mL penicillin and 10,000 μg/mL streptomycin) in an atmosphere of 5 % CO_2 and 95 % relative humidity (RH) at 37 °C. The cytotoxicity of GEM, VES-GEM, blank Soluplus® micelles, and Soluplus®/VES-GEM micelles (prepared as described in section 2.3) was determined, in quadruplicate, using an AlamarBlue assay (ThermoFisher, Waltham, MA, USA). Briefly, cells were expanded till 80 % confluency, trypsinized, and seeded at a density of 2×10^4 cells/well into 96-well plate and incubated for 72 h at 37 °C in a 5 % CO_2, 95 % RH humidified incubator. The formulations were added to the cells in various concentrations, namely 100, 10, 1, 0.1, or 0.01 μM of VES-GEM or equivalent (*i.e.,* Soluplus® blank formulation tested in the same dilution as the VES-GEM-loaded Soluplus® micelles), and the cells were incubated during 72 h, under the same conditions. All formulations were prepared in PBS, except VES-GEM as 100 % DMSO solution. Control was culture medium, and blank was the AlamarBlue kit reagent. Cells were monitored under Nikon Eclipse TS100 microscope, equipped with a DXM 1200 digital camera (Nikon, Tokyo, Japan). Cell proliferation was analysed in accordance with AlamarBlue protocol. In brief, culture medium was withdrawn from the wells, cells were washed with PBS twice, and AlamarBlue working solution was added to each well (150 μL AlamarBlue stock solution diluted in culture medium 1:10 *v/v*) followed by incubation at 37 °C for 2 h. Finally, fluorescence of the supernatants was measured at an excitation wavelength of 540 nm and emission wavelength of 580 nm using a microplate FLUOstar Omega (BMG LABTECH, Germany). Equation (6) was used to calculate cell viability, as follows.

$$Cell\ viability(\%) = \frac{RFU_{exp} - RFU_{blank}}{RFU_{control} - RFU_{blank}} \times 100 \quad (6)$$

RFU_{exp} is sample relative fluorescence units, RFU_{blank} represents the blank (AlamarBlue reaction in medium) relative fluorescence units, and $RFU_{control}$ stands for control relative fluorescence units (AlamarBlue reaction in non-treated cells).

2.11. Cell uptake

Fluorescent-labelled Soluplus® micelles were prepared by adding Nile red solution was prepared in ethanol (0.4 mg/mL; 66.7 μL) dropwise to 2.5 mL Soluplus® micelle dispersions under stirring (250 rpm) in

a hood protected from light. Ethanol was let to evaporate overnight to a final Nile red concentration of ~ 10 μg/mL. BxPC3 cells were cultured as described in section 2.10., collected and seeded on 8-well glass slides (Lab-Tek II chamber slides; Thermo Scientific, Waltham, MA, USA) at a density of 5×10^4 cells/well and incubated overnight. Then, cells were incubated for 2 h with 200 μL PBS-diluted Nile red-loaded Soluplus® micelles (8.5 mg/mL Soluplus®, equivalent polymer concentration to the highest VES-GEM concentration tested *in vitro* for cytotoxicity). BxPC3 cells were then washed with PBS three times, fixed with 4 % paraformaldehyde (100 μL/well) for 10 min, rinsed thrice with PBS, incubated with Triton X-100 (0.2 % in PBS) for 5 min, and washed with PBS again three times. Then, cells were dyed with DAPI ProLong gold antifade (Molecular Probes; Eugene, OR, USA), covered with a glass coverslip, and kept at −20 °C until observation. Confocal laser scanning microscopy (CLSM) analysis was carried out using a Stellaris 8 confocal microscope (Leica Microsystems; Wetzlar, Germany).

2.12. Cell viability in 3D model

The efficacy of the formulations was also evaluated in a 3D *in vitro* model of pancreas ductal adenocarcinoma. To recreate the desmoplasia environment present in this type of tumor, BxPC3-laden collagen hydrogels were used (Shields et al., 2012; Rajan et al., 2006). Collagen type I (Col1) was isolated from rat tail tendons from wastes of bioterium (Rajan et al., 2006), and its concentration was measured by microBCA (Thermo Fisher Scientific) (Blanco-Fernandez et al., 2022). Col1 pre-gel was prepared by neutralizing the dispersion with NaOH 1 M and correcting its osmolarity with DPBS10x. Then, complete cell media containing the cell suspension was mixed to achieve a final Col1 concentration of 4 mg/mL and a BxPC3 cell density of 3×10^6 cells/mL. Afterward, 25 μL of the pre-gels was deposited onto 48-well plates and incubated for 30 min at 37 °C for 15 min. Finally, 300 μL of cell media was added carefully into each well. Cell-laden hydrogels were kept 4 days in culture, replacing the cell media every other day.

The efficacy of VES-GEM and the formulations against BxPC3 was evaluated by AlamarBlue. Briefly, after 4 days in culture, the cell medium was replaced by each formulation diluted in cell medium and incubated 72 h (n = 4) as specified in section 2.10. In contrast, VES-GEM was prepared in DMSO 0.5 % in cell media. The metabolic activity of each tumoroid before and after the treatment was measured by AlamarBlue, by incubating the cell-laden hydrogels with 200 μL of the reagent at 10 % in cell medium for 1 h. Cellular viability was calculated using nontreated hydrogels as negative controls (non-treated or treated with DMSO 0.5 %) and normalizing each value by the metabolic activity before the treatment.

2.13. BxPC3 cell membrane extraction through ultracentrifugation and preparation and characterization of BxPC3 cell membrane-modified Soluplus®/VES-GEM micelles

2.13.1. BxPC3 cell membrane extraction through ultracentrifugation

BxPC3 cell membrane fragments were obtained through hypotonic lysis (Fang et al., 2014; Li et al., 2020; Cao et al., 2021) and differential centrifugation, including two ultracentrifugation steps (Fang et al., 2014). Cells were washed two times with PBS (10 mL) and trypsinized (3 mL, 10 min incubation at 37 °C), and medium (6 mL) was added to block trypsin action. The cell suspension was collected, centrifuged at 300*g* (5 min/4 °C (Sorvall™ Legend™ Micro 21R Microcentrifuge, Thermo Fisher™, Madrid, Spain), washed with PBS (10 mL) and centrifuged again at 300*g* (5 min /4 °C). The washed cell suspension was filtered (Biofil sterilized syringe filter, 30 mm, 0.22 μm PES membrane; Barcelona, Spain), proper for cell materials, and the supernatant was discarded. For hypotonic lysis, hypotonic lysing buffer (2 mM $MgCl_2$, 20 mM Tris-HCl, 10 mM KCl) with 1 % protease inhibitor (phenylmethylsulfonyl fluoride, PMSF) was prepared. Hypotonic buffer (10 mL) was added to the falcon tube containing the cell pellet followed by homogenization with up and down movements. The mixture was incubated for 1 h, protected from light, at 4 °C and was then ultrasonicated using a Branson Digital Sonifier 150 (Branson Ultrasonics, Marshall Scientific, New Hampshire, NH, USA) at 20 % intensity in cycles of 5 s on/2 s off during 1 min. The mixture was then subjected to differential centrifugation protocol. Briefly, the falcon tube was centrifuged at 700*g* at 4 °C for 5 min in order to remove cell debris. Supernatant was collected and ultracentrifuged (Optima XPN-100 Ultracentrifuge, Beckam Coulter, USA) at 20,000*g* at 4 °C for 20 min in order to remove nuclear content. The supernatant was collected and ultracentrifuged 100,000*g* at 4 °C for 1 h to remove residual genetic material and intracellular components. The final pellet containing cell membrane fragments was resuspended in PBS (*ca* 200 μL) and stored at 4 °C for further use.

2.13.2. Characterization of BxPC3 cell membrane fragments

Cell membrane fragments were assessed through CLSM by staining aliquots of resuspended pellets resulting from each centrifugation, namely 0.1 mL, 0.1 mL and 0.02 mL (for 700*g*, 20,000*g*, and 100,000*g*, respectively) with DAPI and 1,1′-dioctadecyl-3,3,3′,3′- tetramethylindodicarbocyanine (DiD) for staining nucleus and lipidic bilayer, respectively. Briefly, 1 mL dye mixture containing 20 μL of DAPI and 5 μL DiD were prepared and preserved from light. Then, 0.330 mL of dye mixture were added to the three aliquots followed by incubation for 30 min (RT) protected from light, mounted on glass slides and visualized using CLSM. Membrane protein content was quantified through Micro BCA™ protein assay kit (Thermo Fisher™, Madrid, Spain). The incubation time (AccuBlock Digital Dry Bath) was 30 min at 37 °C and the absorbance read at 562 nm.

2.13.3. Preparation and characterization of BxPC3 cell membrane-modified Soluplus®/VES-GEM micelles

BxPC3 cell membrane nanovesicles were prepared through sequential extrusion of the membrane fragments suspension in PBS (0.2 mL, 0.5 mg/mL protein content), namely 10 cycles with polycarbonate membrane 400 nm, and followed by 10 cycles with polycarbonate membrane 200 nm. For cell BxPC3 cell membrane coating, different methods were tested, namely 1) sonication of the mixture of Soluplus®/VES-GEM micelles (0.1 mL, 1 mg/mL Soluplus® concentration) and BxPC3 cell membrane nanovesicles (0.2 mL, 0.5 mg/mL protein content) followed by co-extrusion with polycarbonate membrane 200 nm, 10 cycles; 2) co-extrusion of BxPC3 cell membrane nanovesicles (0.2 mL, 0.5 mg/mL protein content) with Soluplus®/VES-GEM micelles (0.1 mL, 1 mg/mL Soluplus® concentration); and 3) ultrasonication (3 min (3 s/1s)) of the membrane fragments suspension (0.2 mL, 0.5 mg/mL protein content) with Soluplus®/VES-GEM micelles (0.1 mL, 1 mg/mL Soluplus® concentration) (**Figure S2**). The formulations were characterized regarding size, ZP, PDI and TEM.

2.14. BxPC3 cell membrane extraction through mild centrifugation, preparation and characterization of BxPC3 cell membrane-modified Soluplus®/VES-GEM micelles

2.14.1. BxPC3 cell membrane extraction through mild centrifugation

BxPC3 cells were collected after achieving 90 % confluency and the membrane fragments were obtained through hypotonic lysis and mild centrifugation according a procedure adapted from Cao et al. (2021) and Zou et al. (2023). Briefly, cells were trypsinized, centrifuged at 1200*g*/4 min (Centrifuge 5417 R Eppendorf AG, Hamburg, Germany) and, then the cell pellet was resuspended in 1 mL hypotonic lysing buffer (10 mM Tris·HCl), 10 mM $MgCl_2$ and 1X EDTA-free protease inhibitor. Hypotonic lysing buffer (a tablet of protease inhibitor in 10 mL PBS 0.25X, followed by addition of Tris and $MgCl_2$ at needed concentrations and the mixture was stirred for 2 h, protected from light. The mixture of hypotonic buffer and cells was incubated overnight in ice with shaking (190 rpm). The mixture containing cell material suspended in the hypotonic

lysis buffer was diluted twice with hypotonic lysing buffer and sonicated, in an ice container, using Sonifier 450 ultrasonicator (Branson Ultrasonics, Marshall Scientific, New Hampshire, NH, USA) frequency 20 kHz, potency 400 W, 117 V, 50/60 Hz, 20 % intensity, 10 times, 5 s on/3 s off cycles. The obtained cell membrane fragment suspension was centrifuged at 3200*g* for 5 min at 4 °C to remove intact cells and cell nucleus, the pellet was reserved for further analysis and the supernatant was collected and divided into two Eppendorf tubes (1.5 mL) centrifuged at 7000*g* for 10 min at 4 °C to remove mitochondrial material. The pellet was reserved, and the supernatant was collected and divided in 2

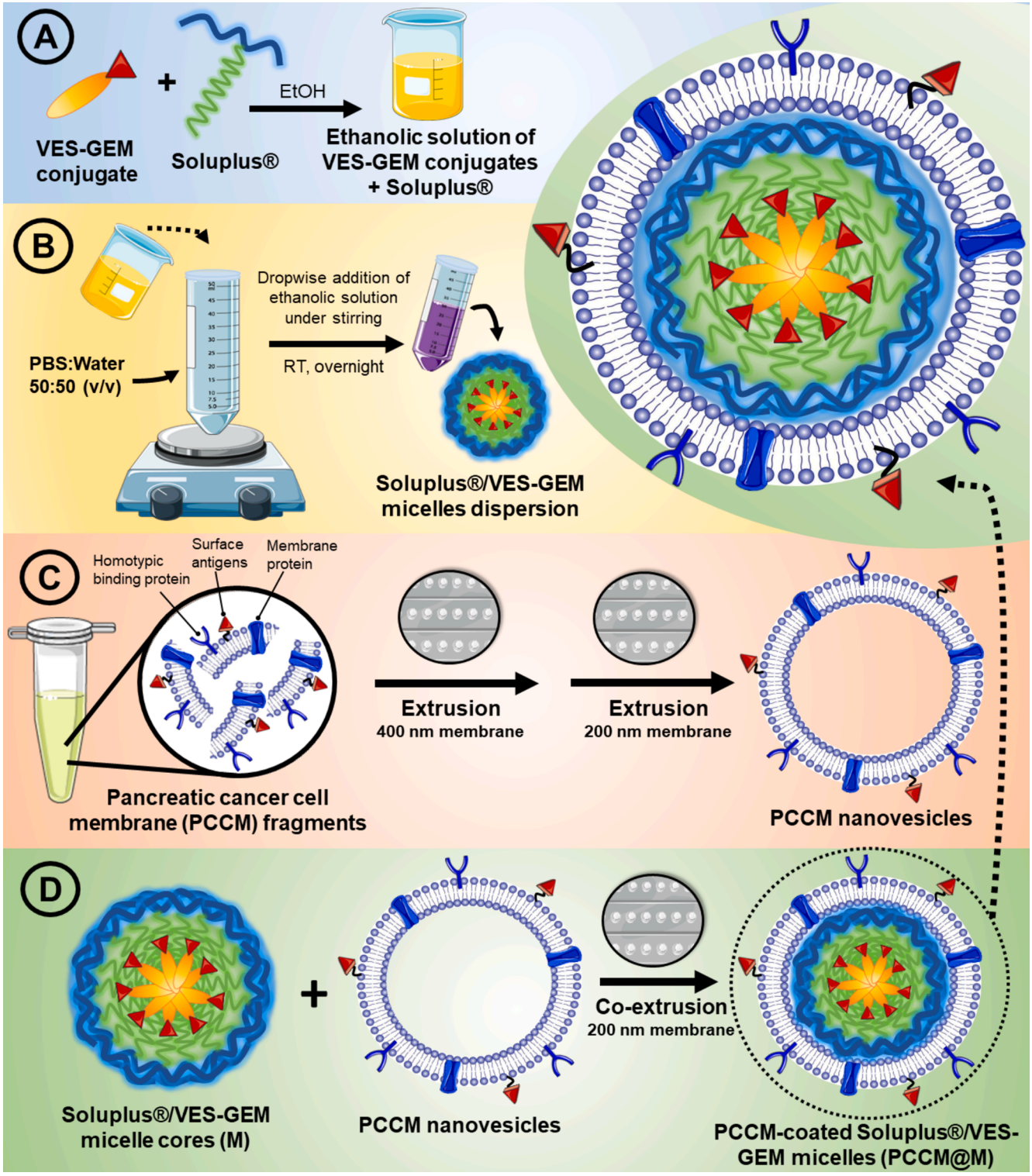

Fig. 2. Preparation of BxPC3 cell membrane-modified Soluplus®/VES-GEM micelles through co-extrusion of BxPC3 membrane nanovesicles with Soluplus®/VES-GEM micelle cores. Soluplus®/VES-GEM micelles were prepared recurring to solvent evaporation method (A, B). Briefly, appropriate amount of VES-GEM conjugate was dissolved in ethanol and added dropwise to 50:50 PBS:water mixture, and left overnight stirring in a hood to enable ethanol evaporation. BxPC3 cell membrane nanovesicles were prepared through extrusion (C) and a mixture of micelle cores with BxPC3 nanovesicles was co-extruded (200 nm pore size) to assemble PC cell membrane (PCCM)-modified Soluplus®/VES-GEM micelles (D).

new Eppendorf tubes (1.5 mL) and further centrifuged at 15,000*g* for 60 min at 4 °C to obtain purified cell membrane fragments as pellet. The membrane pellet was washed twice with 1 mL PBS, decanted without resuspension, then resuspended in 0.5 mL PBS. It was stored at 4 °C for short-term use or at −80 °C for longer storage.

A sample from each centrifugation step was analyzed for genetic material content using a Quant-iT PicoGreen dsDNA assay kit (ThermoFisher, Waltham, MA, USA). The final membrane fragment suspension was quantified for protein content using the Micro BCA™ protein assay kit.

2.14.2. Preparation of cell membrane-modified micelles

Soluplus®/VES-GEM micelles were coated using a serial extrusion procedure with polycarbonate porous membrane (Zou et al., 2023). First, BxPC3 cell membrane nanovesicles were prepared and quantified for protein content using a Micro BCA™ protein assay kit. Then, membrane material was diluted to 1 mg/mL and extruded through 400 nm (10 cycles) and 200 nm membranes (10 cycles). Soluplus®/VES-GEM micelles formulation was diluted 5× with MiliQ® water, and 0.15 mL (Soluplus® concentration 6 mg/mL) were added to 0.190 mL BxPC3 cell membrane nanovesicles and co-extruded using membrane pore 200 nm for 10 cycles, for assembling BxPC3 cell membrane-modified Soluplus®/VES-GEM micelles with a polymer-to-protein weight ratio 6:1. Controls were included to assess the effect of extrusion on Soluplus®/VES-GEM micelles and to compare simple mixtures of BxPC3 nanovesicles with Soluplus®/VES-GEM micelles against the BxPC3-modified micelles. For extruded Soluplus®/VES-GEM micelles, diluted micelles (0.15 mL, Soluplus® concentration 6 mg/mL) were further diluted with Milli-Q® water and extruded through 400 nm and 200 nm membranes (10 cycles each) (Fig. 2).

Soluplus®/VES-GEM micelles and BxPC3 nanovesicles mixture was prepared by adding BxPC3 nanovesicles (0.15 mL) to the extruded Soluplus®/VES-GEM micelles as before (0.3 mL) with gentle homogenization to endow adequate mixing. The final obtained volume for each formulation was diluted with MiliQ® water to 0.7 mL to allow for DLS measurement.

A set of parallel experiments was conducted as before but replacing co-extrusion with ultrasonication of micelle cores with BxPC3 nanovesicles, in ice container, using Sonifier 450 ultrasonicator (10 times, 3 s each, amplitude 10 %) to assess the influence of ultrasonication on the fabrication of coated micelle cores. Controls were ultrasonicated Soluplus®/VES-GEM micelles and a mixture of Soluplus®/VES-GEM micelles and BxPC3 nanovesicles.

2.14.3. Titration of Soluplus®/VES-GEM micelle cores with BxPC3 cell membrane nanovesicles

To reduce membrane material needed for coating and to optimize the coating procedure, a titration of Soluplus®/VES-GEM micelle cores with increasing concentrations of BxPC3 membrane (expressed in protein mg/mL) was carried out for studying the influence of the amount of membrane material employed for coating of Soluplus®/VES-GEM micelle cores. For that, the procedure followed the methodology explained in 2.13.3, namely 0.2 mL of BxPC3 membrane nanovesicles with distinct protein concentrations were co-extruded with 0.2 mL of Soluplus®/VES-GEM micelle cores with specific polymer and VES-GEM concentrations (**Table S3**).

2.15. Characterization of BxPC3 cell membrane-modified Soluplus®/VES-GEM micelles

2.15.1. Hydrodynamic size, PDI, ZP and morphological evaluation

The hydrodynamic size, PDI and ZP of the different formulations were measured by DLS, as described above (n = 3). Morphological evaluation of the BxPC3 cell membrane nanovesicles and BxPC3 cell membrane-modified Soluplus®/VES-GEM micelles were evaluated by TEM, as described above.

2.15.2. Co-localization

Soluplus® micelle core was dyed with Nile red, and BxPC3 cell membrane-nanovesicles with dye-labelled phospholipid DOPE-Atto 488, which is able to intercalate in the lipid bilayer of cell membrane nanovesicles through hydrophobic effect (Soprano et al., 2020). Briefly, 100 μL of stock solution of Nile red in ethanol (0.4 mg/mL) was added dropwise to a Soluplus® dispersion in PBS (3.75 mL, 29.8 mg/mL Soluplus® concentration) and left overnight to evaporate organic solvent, protected from light, in a hood. The next day, the Nile red-loaded Soluplus® micelles were transferred to a dialysis bag, sealed and dialysed against MiliQ® water for 24 h at RT, protected from light, and the medium was replaced frequently to allow diffusion of non-loaded Nile red. The resulting Nile red-loaded Soluplus® micelles were collected and kept at RT for further use. DOPE-Atto 488-labelled BxPC3 cell membrane-nanovesicles were prepared by adding 1 μL of a stock solution of DOPE-Atto 488 (1 mg/mL, in DMSO) to 200 μL of membrane fragments mixture (1 mg/mL protein content) and the mixture was extruded through 400 nm and 200 nm membranes, 10 cycles each, and the formulation was dialysed as previously described. Nile red-loaded Soluplus® micelles (0.1 mL) were co-extruded with DOPE-Atto 488-labelled BxPC3 cell membrane-nanovesicles (0.1 mL) through 200 nm membrane, 10 cycles, and the obtained DOPE-Atto 488-labelled BxPC3 cell membrane-modified Nile red-loaded Soluplus® micelles were placed at 4 °C, protected from light, for further use. For CLSM analysis, the sample was mounted in glass slides using SlowFade™ Diamond Antifade Mountant (Invitrogen™, Thermo Fisher™, Madrid, Spain) to increase fluorescence signal and kept at −20 °C for further CLSM analysis.

2.15.3. Cell viability in 2D and 3D models

Cell viability tests with the BxPC3-modified formulation were carried out as described in section 2.10 and 2.12.

2.16. Statistical analysis

Statistical data analysis was carried out using GraphPad® Prism® 10.1.2 (San Diego, CA, USA). All results were expressed as mean ± standard deviation, when applicable. Results were analysed using ANOVA followed by *post hoc* Tukey honest significance test, when appropriate. For statistical significance, values < 0.05 were considered.

3. Results and discussion

3.1. Preparation and characterization of Soluplus®/VES-GEM micelles

Soluplus® was chosen due to its ability to self-assemble in aqueous environment forming highly stable, biocompatible micelles (CMC *ca.* 0.0003 mM; Bernabeu et al., 2016) with hydrophilic shell, which can prolong blood circulation of VES-GEM conjugate by minimizing immune uptake and improving pharmacokinetics. A starting concentration of 3 % *w/v* of Soluplus® was selected based on previous studies (Bernabeu et al., 2016) and a near 1/1 polymer-to-conjugate mole ratio (Xu et al., 2015).

The VES-GEM conjugate was synthesised recurring to amidation reaction established between amine group of GEM and succinate moiety of VES, and characterized as reported before (Pereira-Silva et al., 2024). The VES-GEM conjugate had very low water solubility ($\ll 0.01$ mg/mL), logP of 8.93 and non-ionized form predominated at physiological pH (Pereira-Silva et al., 2024), hence encapsulation process was mainly driven by the presence of hydrophobic substitutions of VES-GEM. VES-GEM was suggested to be internalized efficiently in the hydrophobic core of Soluplus® micelles composed of hydrophobic polyvinyl caprolactam–polyvinyl acetate blocks assembling compact micelles with typical larger size when compared to other polymers displaying lower MW, as expected. Theoretically, it is expected hydrophobic interactions established between hydrophobic segments of Soluplus®, a grafted

polymer, and VES alkyl chain and cyclic central ring system to be major drivers of intermolecular interactions enabling the encapsulation of VES-GEM, together with hydrogen bonding established between –OH and –F groups of GEM and the hydrophobic polymer backbone (terminal –OH residues and ether groups) (Piazzini et al., 2019). Electrostatic and π- π are not expected to prevail due to absence of ionized groups and aromatic rings' systems.

3.1.1. Low polymer-to-conjugate ratios

First, a set of experiments exploring the lower range of polymer-to-conjugate mole ratio to reduce maximum amount of excipient needed for VES-GEM solubilization was carried out, fixing VES-GEM concentration (0.4 mg/mL). Both 0.45 % NaCl and PBS:water (50:50 *v/v*) media were tested to assess the influence of medium composition on physical properties of micelles. After evaporation of ethanol, the formulations showed large aggregates, and the size, ZP and polydispersity index were recorded after filtration with 0.4 μM PTFE filter (**Table S4**).

The pH of the formulations tested in 0.45 % NaCl and PBS:water (50:50 *v/v*) media varied from acidic (pH < 4) to slightly alkaline (pH > 7.0), respectively, suggesting PBS buffering. This is in accordance to literature as aqueous Soluplus® solutions are typically acidic (Bernabeu et al., 2016). Lower pH resulted in smaller micelles, especially in 0.45 % NaCl. ZP values were near 0 mV, attributed to Soluplus® hydrophilic shell (Xu et al., 2015). Regarding Soluplus®/VES-GEM micelles prepared in hypotonic PBS medium, the transition from slightly negative-charged micelles with 0.14/1 ratio to slightly positively charged surface of micelles bearing 0.30/1 ratio could be attributed to increased ionic strength of the medium. High polydispersity (PDI > 0.4) suggested that all formulations were prone to aggregation.

Two quantification methods were employed to assess the drug content in Soluplus®/VES-GEM micelles: direct detection of VES-GEM conjugate and alkaline hydrolysis to quantify free GEM (Khare et al., 2016; Sun et al., 2020) (**Table S5**). Micelles with a 0.14/1 mole ratio exhibited the highest encapsulation efficiency (EE) in both hypotonic NaCl and PBS media. EE of GEM followed a similar trend, with higher efficiency observed for the 0.14/1 Soluplus/VES-GEM formulation. Direct quantification of VES-GEM proved more efficient in measuring drug-loaded micelles compared to alkaline hydrolysis for free GEM quantification. Drug loading increased with higher Soluplus/VES-GEM mole ratios but remained near or under 5 % w/w due to the high average molecular weight of Soluplus®.

3.1.2. Increasing polymer-to-conjugate mole ratios

The previous formulations were not stable at RT, evidenced by the formation of large precipitates after preparation when left unstirred. To address this, a set of formulations were prepared in PBS:water (50:50 *v/v*) to investigate the effect of increasing Soluplus® concentration on the preparation of Soluplus®/VES-GEM micelles with higher polymer-to-conjugate mole ratios (Table 1**, Figure S3**).

Results showed filtered Soluplus®/VES-GEM micelles with mole ratio 0.5/1 displayed the smallest size (*ca.* 88 nm) and were less polydisperse than the other formulations (**Figure S3 A, C**) evidenced a spherical structure (**Figure S3 D**). Increased Soluplus® concentrations led to a non-relevant increase in ZP values (**Figure S3 B**). Soluplus®/VES-GEM micelles bearing 0.5/1 mole ratio showed better stability for at least 7 days (by means of reduced visually detected precipitation and aggregation) and were prepared with lower Soluplus® concentrations (29.8 mg/mL) when compared to 1/1 and 1.5/1 mole ratios. Ethanolic mixtures of Soluplus®/VES-GEM bearing ratios above 1.5/1 resulted in highly viscous gel-like solutions and hampered subsequent dropwise addition to the medium.

3.1.3. Decreasing conjugate concentration

Then, the formulation was optimized by reducing VES-GEM concentration to 4 mg in order to improve overall stability and decrease unloaded VES-GEM (polymer-to-conjugate mole ratio 0.75:1, VES-GEM concentration 0.267 mg/mL). Optimized Soluplus®/VES-GEM micelles (0.75/1) presented a size of *ca.* 100 nm **(**Fig. 3 **A, E-F)** and nearly neutral charge **(**Fig. 3 **B)** and narrow particle size distribution **(**Fig. 3 **C)** consistent with previous findings (Bonde et al., 2020). Notably, Soluplus/VES-GEM (0.75/1) formulation showed enhanced colloidal stability, with no visible precipitate or agglomeration after preparation (Fig. 3 **D**) or stored unstirred at RT for over a month. Additionally, TEM micrographsconfirmed spherical nanoparticles with size 100–200 nm **(**Fig. 3 **E, F).**

Soluplus/VES-GEM micelles (0.75/1 mole ratio) prepared in PBS: water (50:50 *v/v*) medium were able to encapsulate the majority of VES-GEM in the non-purificated system; EE(%) = 97.55 ± 2.28; DL(%) = 0.931 ± 0.022. The low drug loading observed was related to the high concentrations of Soluplus® used in this study and to the high molecular weight of the polymer (115,000 g/mol). The solvent evaporation method showed good reproducibility and may be comparable to other methods such as film hydration (TFH) method, used to produce structures with uniform size and monodisperse population (Bonde et al., 2020; Lim et al., 2023). While some authors have developed centrifugation protocols to eliminate unloaded drug, maintaining micelle structure integrity poses a challenge, potentially resulting in incomplete precipitation of free drug aggregates (Lim et al., 2023). Soluplus®/VES-GEM (0.75/1) micelles showed no significant change in EE after centrifugation at 4000 rpm/30 min/RT (EE(%) = 98.62 ± 3.49), suggesting nearly complete drug encapsulation in the micelles.

Increasing the centrifugation speed to 12,000 rpm for 20 min resulted in a decrease in EE(%) to 78.87 ± 5.98, indicating the potential elimination of unloaded VES-GEM. The formation of a pellet after centrifugation suggested possible collapse of the micelle structure or polymer aggregation. Centrifugation was not pursued further due to concerns about stability loss and uncertain elimination of free VES-GEM, as well as the risk of early drug release (Mahmud et al., 2024). Filtration (pore size of 0.4 μM) eliminated most of the VES-GEM from the micelles (EE(%) = 0.95 ± 0.14), likely due to filter clogging with polymer and formulation (size ~ 100 nm), making it an unsuitable method for selective elimination of unloaded drug. Dialysis, although commonly used for micelle system purification, was not explored further due to the potential risk of unwanted drug release (Wang et al., 2020).

Recent studies have explored ultrafiltration as an alternative purification method, leveraging centrifugal forces to separate unloaded drug by size. After brief ultracentrifugation with Amicon Ultra 0.5 mL Centrifugal filters (100 kDa) at 1000 rpm for 3 min at 25 °C, initial drops of the formulation were collected to estimate the amount of unencapsulated VES-GEM, as micelles would be retained in the filter compartment due to their size. Short centrifugation time and speed were selected for establishing the extension of VES-GEM encapsulation in Soluplus® micelles by assuming concentration of free VES-GEM was the same in the ultrafiltrate drops and in the upper compartment (Marques et al., 2020). Results showed that the formulation compartment had ~ 80 % of VES-GEM, suggesting that a significant amount of VES-GEM is non-encapsulated and that EE(%) is lower than that observed without any purification (**Table S6**).

The results suggest that the accuracy of estimating unencapsulated VES-GEM with the first collected drops is uncertain, and their representativeness of the formulation medium composition without interference with the micelle systems is unclear. Although ultrafiltration offers potential for complete system purification, challenges such as membrane filter clogging, drug aggregate formation, and early drug release need to be addressed (Tehrani et al., 2023).

Besides elimination of free drug and agglomerates that form during or after preparation of the formulation, the purification of the system by elimination of unwanted excessive surfactant is also relevant and should not be discarded (Ruiz et al., 2024). For the Soluplus®/VES-GEM (0.75/1) micelles, the presence of free Soluplus® is hard to predict due to the nature and limitations of the system. The right purification method may depend largely on the type of nanosystem, polymer used, drug used and

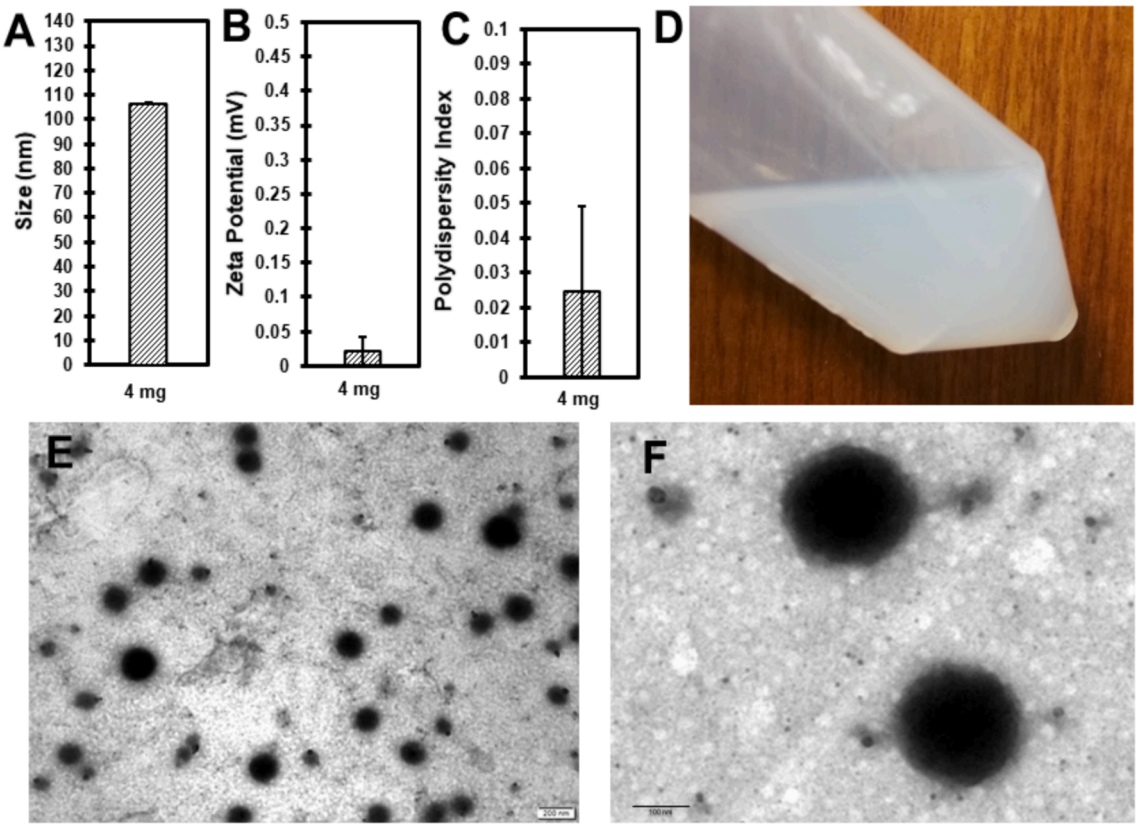

Fig. 3. (A) Size, (B) zeta potential, (C) polydispersity index, and (D) physical appearance of Soluplus/VES-GEM micelles (0.75/1 mole ratio) dispersion prepared in PBS:water (50:50 *v/v*) medium. Samples were filtered for DLS measurements using 0.4 μM PTFE filter. (E, F) TEM images of non-filtered Soluplus/VES-GEM micelles (0.75/1 mole ratio), in PBS:water (50:50 *v/v*) medium. Scale bar: (E) 200 nm and (F) 100 nm.

stability of the system (Tehrani et al., 2023).

Soluplus®/VES-GEM (0.75/1) micelles were further visualised through FESEM (**Figure S4 A-C**) and showed spherical structures with irregular surfaces, and sizes between 100–300 nm. Two different batches of formulation were prepared and tested after filtration (0.4 μM) and after centrifugation (**Figure S4 D-F**). Without purification, the two batches showed some variability in size and PDI, which was reduced after filtration and centrifugation, more pronounced to the batch subjected to 12,000 rpm centrifugation speed.

Additionally, Soluplus®/VES-GEM (0.75/1) micelle formulation exhibited characteristic absorption peaks of VES-GEM at 269 nm attesting the successful assembly of VES-GEM with Soluplus® (**Figure S4 G**). CMC of Soluplus® was observed to be < 0.1 mg/ml which is in accordance to previously reported values (Alambiaga-Caravaca et al., 2020). Importantly, the presence of VES-GEM did not significantly impact the self-assembly behaviour of Soluplus® (**Figure S4 H).**

For solubility studies, micelles prepared with different increasing VES-GEM concentration, with fixed Soluplus® concentration, were subjected to centrifugation (Alambiaga-Caravaca et al., 2020; Varela-Garcia et al., 2018; Vivero-Lopez et al., 2022) (**Table S7**). Centrifugation of VES-GEM containing Soluplus® micelles resulted in significant precipitation at VES-GEM concentrations of 0.2 mg/mL and above when subjected to 4000*g*/30 min. This trend indicates that as the VES-GEM concentration increased, the Soluplus®/VES-GEM micelles became more hydrophobic, leading to decreased apparent solubility and destabilization of the system, facilitating precipitation. Considering these results, it is challenging to ascertain the solubility of VES-GEM as a function of Soluplus® concentration. Nevertheless, the high EE of VES-GEM (>80 %) in non-centrifuged formulation suggested that the solubility in 29.8 mg/mL of Soluplus® may be near the concentration of VES-GEM used (0.267 mg/mL). Future studies need to explore alternative methods to quantify VES-GEM solubility in Soluplus® and examine the interactions between the polymer and the conjugate, such as filtration, not explored here due to the previously attested limitations (Rao et al., 2024).

3.2. *VES-GEM release*

Soluplus®/VES-GEM micelles (0.75/1) showed no appreciable release after 3 days of incubation (37 °C, 180 rpm) of 1 mL of formulation (29.8 mg/mL Soluplus®; 0.267 mg/mL VES-GEM). After 7 days, no release was verified. By contrast, high concentrations of VES-GEM were detected inside the dyalisis membrane after 7 days of incubation (0.155 ± 0.01 mg/mL and 0.200 ± 0.01 mg/mL for pH 7.4 and pH 5, respectively). Various parameters were tuned to investigate their effect on the VES-GEM release profile, including release medium composition, volume, surfactant type and concentration, and dialysis membrane characteristics (Table 2).

Tween 80 0.5 % *v/v* was chosen as main surfactant based on previous studies investigating the release of GEM lipidic prodrugs. The chosen dialysis bag with a MWCO of 12,400 was sufficiently large to facilitate the release of VES-GEM without membrane saturation yet small enough to prevent the passage of Soluplus® micelles. Other studies have shown mild release of lipidic prodrugs from nanosystems (Abouelmagd et al. 2015), namely DSPE-PEG/TPGS mixed micelles encapsulating prodrug C_{18}-GEM achieving only 50 % release of prodrug after 12 h (dialysis against PBS buffer, dialysis bag MWCO 20 kDa) (Wang et al., 2014), and C_{18}-GEM-loaded PEG/PLA micelles showed < 30 % release of C_{18}-GEM after 72 h period, even in presence of Tween 80 0.5 % *v/v* (Daman et al., 2014). Soluplus® micelles containing idebenone and miconazole also showed low drug release (<20 % for both drugs) even in medium supplemented with ethanol or methanol (30 % *v/v*) (Pignatello et al., 2022).

This slow release effect was also observed in other studies with Soluplus® micelles as drug carriers (Dong et al., 2023). Moreover, the high stability of the amide bond, along with the overall stability of the VES-GEM system developed in this study, suggests that GEM activity could be extended over time under physiological conditions. This slow-release mechanism, facilitated by enzymatic cleavage through cathepsin B, amidases, phospholipases, esterases, or by hydrolysis, ensures a prolonged availability of GEM, enhancing its therapeutic activity ensuring its stability (Bildstein et al., 2011; Bulanadi et al., 2020; Kakwere et al., 2020).

The absence of VES-GEM release was not expected since the membrane dialysis was washed and conditioned as per manufacturer's guide, and sink conditions were assured (Pereira-Silva et al., 2024). The lack of transference to the medium outside the dialysis bag may be related to the extreme lipophilicity nature of VES-GEM. Additionally, it shows that Soluplus®/VES-GEM micelles (0.75/1) accommodate and retain VES-GEM conjugate for long periods of time, which may be beneficial for *in vivo* applications demanding long-acting GEM depot for long treatment period. The interactions established between the polymeric backbone and VES-GEM, allied with the hydrophobicity of VES-GEM, may render Soluplus®/VES-GEM micelles (0.75/1) with improved VES-GEM retaining properties and suggest a highly stable colloidal system with low propensity to enable drug diffusion (Zhou et al., 2022). It is expected that *in vivo* the conjugate can be cleaved and release GEM and VES, potentially through enzymatic activity, such as cathepsin B (Gaudin et al., 2016; Li et al., 2023), esterases (Bulanadi et al., 2020) and amidases (Wu et al., 2020). Collectively, these results support the argument that Soluplus®/VES-GEM micelles (0.75/1) are both thermodynamic and physiochemically stable and promising suitable GEM carriers for further *in vitro* studies.

3.3. Stability of Soluplus®/VES-GEM micelles (0.75/1)

3.3.1. Physical and chemical stability at 4 °C and 37 °C

Soluplus®/VES-GEM micelles at a ratio of 0.75/1 were stable at both 4 °C and 37 °C for 27 days, showing no appreciable changes in pH, size, zeta potential or PDI (**Figure S5 A-D**), in agreement with literature (Jin et al., 2020). The visual appearance of the formulations changed noticeably when exposed to 37 °C, resulting in a milkier appearance compared to the more translucent appearance observed at 4 °C (**Figure S5 E**) and could be related to the temperature-dependent self-assembly process of Soluplus® micelles, which may lead to in situ gelling (Rodriguez-Evora et al., 2014).

Soluplus®/VES-GEM micelles showed an ability to maintain constant VES-GEM content throughout 4 weeks (~0.15 mg/mL). Regarding GEM content, quantified by alkaline hydrolysis, the formulations incubated at 37 °C revealed less GEM concentration when compared to those stored at 4 °C, suggesting temperature may impact the hydrolysis procedure and render inferior GEM released (**Figure S5 F,G**).

3.3.2. Stability upon dilution, in protein corona-mimicking conditions and batch-to-batch variation

After *in vivo* administration, micelles are exposed to blood circulation and the effect of dilution. Therefore, Soluplus®/VES-GEM micelles (0.75/1) stability was evaluated after 1:1000 *v/v* dilution in PBS of original Soluplus® and Soluplus®/VES-GEM micelles (**Table S12**). Both Soluplus® and Soluplus®/VES-GEM micelles exhibited particles with a size of 72.39 ± 0.51 nm (PDI: 0.189 ± 0.012) and 70.60 ± 3.38 nm (PDI: 0.224 ± 0.078), respectively, consistent with previous observations for non-diluted Soluplus® blank micelles. The dilution caused a decrease in size of Soluplus®/VES-GEM micelles but an increase in PDI and size distribution intensity mode (%) (**Figure S6 A**) and in number mode (%) (**Figure S6 B**).

PEG-bearing micelles, including Soluplus®, typically have a neutral charge and very hydrophilic shell, making them less likely to be coated by protein corona. However, the extent of protein corona formation on micelles and the underlying mechanisms, especially across different polymer types, remain relatively unexplored (Wang et al., 2022). Soluplus® micelles were incubated with BSA under stirring and size was maintained ~ 80 nm after 24 h (**Figure S6 C**). However, PDI increased substantially (**Figure S6 D**), probably indicating the presence of both BSA nanoparticles and Soluplus® micelles in the sample. Although Soluplus® micelles are thought to interact with serum proteins, the coating of BSA onto the micelles was challenging to detect in this experiment. No relevant changes in zeta potential were recorded either (**Figure S6 E**). This difficulty could be attributed to the high concentration of Soluplus® used (8 mg/mL), which might have compensated for any changes in the zeta potential of the micelles induced by BSA (He et al., 2023; Luo et al., 2022). Given these observations and the strong steric stability conferred by the hydrophilic PEG coating, further exploration of the protein corona effect on VES-GEM-loaded micelles was not pursued in this study.

Two batches were prepared as previously described to ensure the reproducibility of the formulation process and assess batch-to-batch consistency (**Table S8**). The analysis of size and PDI revealed slight differences between the batches, indicating some variability in the preparation process. This variability could be attributed to the dynamic nature of micelles as self-assembled systems, influenced by factors such as temperature, pH, volume of formulation, stirring rate, and ethanol evaporation. Occasionally, a population larger than 500 nm was observed, contributing to an increased PDI (>0.3) (**Figure S6 F**). However, when the batches were analyzed based on distribution by number (%), the size variability appeared more uniform, suggesting that while larger structures may form during the process, their impact in terms of number was minimal (**Figure S6 G**).

3.4. In vitro cell studies

Cell cytotoxicity was carried out on BxPC3 cells incubated in the presence of the developed formulations. Results showed Soluplus®/VES-GEM (0.75/1) were efficient at reducing the cell viability, achieving < 50 % viability for concentrations as low as 1 μM VES-GEM and 27.78 ± 2.75 % for 100 μM VES-GEM concentration, compared to negative control (cell culture medium, $p < 0.05$) (Fig. 4 **A**).

Soluplus®/VES-GEM (0.75/1) micelles exhibited comparable results for cell viability to VES-GEM conjugate for concentrations of 0.1, 1, 10 and 100 μM. This is in full agreement to literature reporting micelles encapsulating lipid-GEM conjugates for PC and other cancer types (Daman et al., 2014; Di et al., 2017; Emamzadeh et al., 2018; Guo et al., 2020; Norouzi et al., 2020; Wang et al., 2014). Studies have also shown GEM prodrugs encapsulation in micelles can improve their cytotoxicity, by IC_{50} reduction, when compared to free GEM and GEM prodrug (Emamzadeh et al., 2018; Norouzi et al., 2020). In this work, the lowest IC_{50} values were reported for VES-GEM control (<0.1 μM), significantly lower that the IC_{50} of GEM of 1.941 μM and the encapsulated system both modified with BxPC3 or not exhibited intermediate results (0.1 < 1 μM) which evidence the suitability of VES-GEM and the VES-GEM loaded micelles as interesting approaches for PC therapy considering the *in vitro* setting (Fig. 4 **C, D**). The ability of Soluplus® to solubilize hydrophobic drugs, improve stability and therapeutic efficiency has been shown in previous reports (Attia et al., 2023; Riedel et al., 2022; Twal et al., 2024; Wang et al., 2020). In this work, the enhanced biocompatibility, small size, accompanied by high physicochemical stability, namely the capability to maintain size, PDI and surface charge constant through a period of 4 weeks, as well as GEM and VES-GEM content, attests the suitability of Soluplus® micelles as carriers for VES-GEM, a hydrophobic GEM prodrug. As a grafted copolymer, Soluplus® possesses a considerably hydrophobized core with high density of vinyl caprolactam and vinyl acetate ramifications, which, together with the low CMC, enables easy micelle formation and accommodation of highly hydrophobic drugs through string hydrophobic interactions, at the same time with hydrophilic periphery by PEG, enabling enhanced

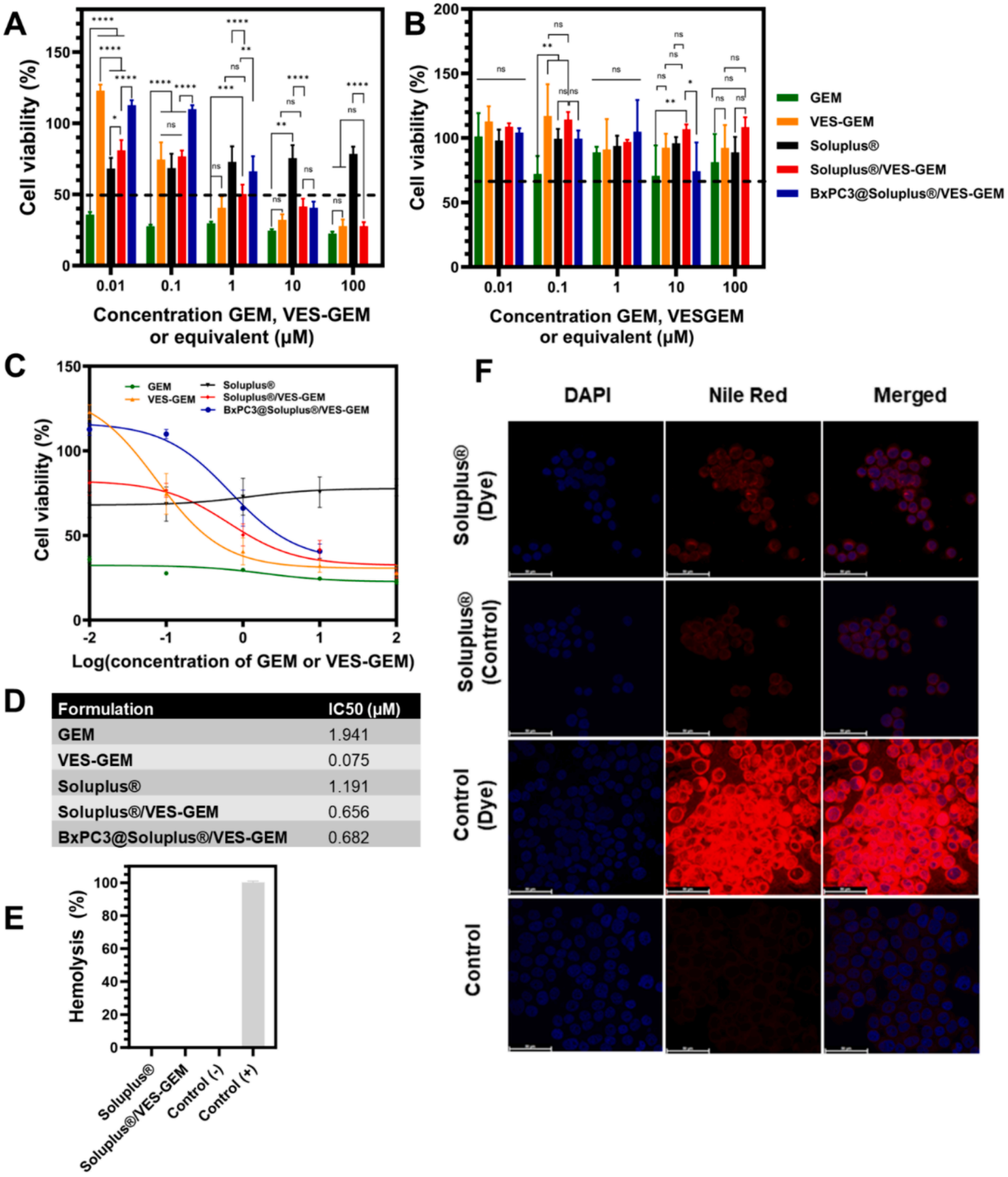

Formulation	IC50 (μM)
GEM	1.941
VES-GEM	0.075
Soluplus®	1.191
Soluplus®/VES-GEM	0.656
BxPC3@Soluplus®/VES-GEM	0.682

Fig. 4. *In vitro* cytotoxicity of GEM, VES-GEM, Soluplus®, Soluplus®/VES-GEM (0.75/1) and BxPC3 cell membrane-modified Soluplus®/VES-GEM (0.75/1) at various concentrations (0.01 μM, 0.1 μM, 1 μM, 10 μM, 100 μM), in BxPC3 cell line model (A) and BxPC3/collagen hydrogel 3D model (B), expressed as cell viability (%) using AlamarBlue assay kit. Dilutions were made in cell culture medium. BxPC3 cell membrane-modified micelle group was tested I concentration range of 0.01–10 μM; (C) IC_{50} curves and (D) IC_{50} values of the formulations GEM, VES-GEM, Soluplus®, Soluplus®/VES-GEM (0.75/1) and BxPC3 cell membrane-modified Soluplus®/VES-GEM (0.75/1) micelles. (E) Haemolytic activity for Soluplus® and Soluplus®/VES-GEM conjugate micelles (0.75/1) in PBS: water 50:50 *v/v*. VES-GEM stock solution was prepared in DMSO and GEM, Soluplus® and Soluplus®/VES-GEM were prepared in PBS. Dilutions were made in cell culture medium. (F) Cellular uptake of Soluplus® micelles showing cell nuclei dyed with DAPI and the micelles were dyed with Nile red (scale bar is 50 μm). Controls were cells stained with Nile red and cells with culture medium. * $p < 0.05$, ** $p < 0.01$, *** $p < 0.001$, **** $p < 0.0001$ (**Table S9, S10**). (For interpretation of the references to color in this figure legend, the reader is referred to the web version of this article.)

solubilization in biological environments.

The cells tested with parent drug (GEM) showed the greatest decrease in cell viability for all concentrations, which is in accordance to previous reports in which C_{18}-GEM-loaded micelles were tested in Panc-1 cell line (range 1–100 μM) (Daman et al., 2014). However, the difference was reduced for higher tested concentrations, namely 100 μM, in the case of VES-GEM and, more importantly, of Soluplus®/VES-GEM (0.75/1) micelles. This elicits the capacity of Soluplus® to solubilize

VES-GEM and increase its encapsulation efficiency, stability and delivery to PC cells by acting as efficient GEM delivery systems with considerable capacity to inhibit cell viability at higher concentrations and comparable to the parent drug. Superior GEM activity is probably attributed to its more activated state which, in the case of the VES-GEM conjugate, GEM is not readily available and needs to be released from the prodrug system. Furthermore, the high stability of the amide bond and the controlled, slow release expected from the prodrug design, vastly undermines the release and therapeutic activity in the 2D model attending to the duration of the experiment, which is even more substantial and time-limited in the case of encapsulation in highly stable Soluplus® core, attested by the absence of noticeable release. The strong ability of Soluplus®/VES-GEM micelles to decrease cell viability is notorious and elicit the ability of the system to function as GEM reservoir for improved GEM therapeutic delivery. Additionally, the high water solubility can also promote efficient uptake of GEM by cells thereby decreasing their cell viability extensively, contributing to the obtained results and in accordance to the literature (Wang et al., 2016), which is distinct for another study that exhibited less action for the free GEM group on account of low cell permeability of GEM (Di et al., 2017). For the concentration of 0.01 μM, the difference between Soluplus®/VES-GEM and GEM was not statistically significant, which may be due to the conferred stability of VES-GEM in the hydrophobic core of Soluplus®, and protection against enzymatic activity of cytidine deaminase (Guo et al., 2020).

Regarding free VES-GEM, the cell viability was similar to Soluplus®/VES-GEM for concentrations of 1, 10 and 100 μM. However, Soluplus®/VES-GEM activity may be superior *in vivo*, as VES-GEM is hydrophobic and its incorporation in Soluplus® micelles can dramatically improve its solubility, stability, release profile and circulation half-life.

Blank Soluplus® micelles showed significant compatibility across all range of concentrations but could elicit mild cytotoxicity effect when compared to control, at concentrations of 11.2 mg/mL (100 μM VES-GEM) and 1.12 mg/mL (10 μM VES-GEM). At lower concentrations, the mild cytotoxic activity could be attributed to the action of free Soluplus® unimers. Soluplus®/VES-GEM micelles revealed to be mostly comparable to free GEM group (<25 % in cell viability at 100 μM) which evidence their ability to function as efficient GEM-containing platforms for drug delivery to PC cells. The BxPC3 membrane-modified micelles showed unexpectedly a tendency to display increased cell viability in the 2D model when compared to the non-modified system, which may indicate the presence of the membrane fragments may stabilize the system and preclude GEM release and activity. Another complementary explanation may be attributed to the unclear surface repertoire disposition and orientation, and electrostatic repulsion exhibited between the negatively-charged membrane fragments shielding the surface of the micelles and negatively-charged membranes.

The cell viability results in the 3D model are shown in Fig. 4 **B**. In general, cells were less sensitive to the formulations tested, which suggests that the 3D model may have already acquired some degree of resistance to the therapy, as GEM control did not provoke any cell dead and micelle diffusion is reduced into the cell-laden hydrogel (Longati et al., 2013). Nevertheless, the 3D tumoroids showed statistically significant cell viability reduction for the BxPC3-modified formulation at the highest concentration tested (10 μM) which may indicate that the modification with BxPC3 membrane may improve the targeting and uptake of GEM in more realistic settings.

Soluplus®/VES-GEM micelles showed no detectable haemolytic activity (Fig. 4 **E**) which corroborates their potentiality as suitable delivery system to PC therapeutics. Several studies have reported efficient cellular internalization of single and mixed Soluplus® micelles (Ding et al., 2018; Dong et al., 2023; Twal et al., 2024), especially when compared with free drug (Jin et al., 2015). In the BxPC3 cell line model, Soluplus® micelles showed only moderate cellular internalization, which may suggest the system may not encapsulate the dye efficiently (Fig. 4 **F**). Some reports use coumarin-6 (Twal et al., 2024) or even drugs that bear fluorescence, such as doxorubicin (Jin et al., 2015). The duration of the cellular internalization may also have impacted, as some studies analyse cell uptake with greater extension of time (Bernabeu et al., 2016; Feng et al., 2020). The small size of Soluplus®/VES-GEM (<100 nm) may contribute to enhanced cellular uptake, on account of easier penetration in the cell membrane, as described before (Dong et al., 2023). However, slightly negative surface charge may hamper its efficient uptake, taking into account the negatively charged surface of cell membranes (Feng et al., 2020). It is possible that Soluplus®/VES-GEM micelles may be internalized and enable GEM release intracellularly, as a blank micelle was used for cell uptake studies in order not to influence cell conditions. The micelles could also release VES-GEM extracellularly, which could penetrate into the cells by diffusion aided by its hydrophobic properties. These results also pave the way to the development of mixed surfactant systems, as reported in the case of Soluplus®/TPGS mixed micelles for paclitaxel delivery, in which single Soluplus® micelles showed both low cellular uptake and cytotoxic activity, which could be leveraged by incorporation of TPGS (Bernabeu et al., 2016).

3.5. Cell membrane extraction through ultracentrifugation, and preparation and characterization of BxPC3 cell membrane-modified Soluplus®/VES-GEM micelles

Cell membranes were successfully extracted in accordance to a hypotonic lysis method followed by differential centrifugation (700*g*, 20,000*g*, 100,000*g*). Instead of extending lysis period, the cells were sonicated first with bath sonicator (4 °C) for 5 min, which revealed insufficient for lysing cell membranes: Differently, the use of an ultrasonicator allowed efficient cell disruption. Aliquots (10 μL) of the resuspended product obtained after 700*g*, 20,000*g*, and 100,000*g* centrifugation were visualized through CLSM. After 700*g* intact and inflated cells and nucleus were observed but no free membrane fragments (**Figure S7 A, B**). The 20,000*g* sample contained free nucleus fragments and no free membrane fragments, in accordance to the theoretical expected results as it should contain less cells and more nuclear material. The 100,000*g* sample contained few free membrane fragments (**Figure S7 C, D**) and free nucleus fragments. Once 100,000*g* resuspended product was not washed with PBS and centrifuged, it may contain cell remnants and the presence of nuclear material is explained. The reduced number of membrane fragments may be due to reduced volume used from the main 100,000*g* Eppendorf, and consequent dilution step resulting from dye solution addition. Quantification of membrane protein through BCA assay showed 3.9 mg/mL protein concentration (**Figure S7 E**), which was dependent on the volume of PBS used to resuspend the membrane pellet.

Due to its simplicity, ultrasonication of micelle cores with membrane fragments was pursued, at 1:1 polymer-to-membrane weight ratios. Ultrasonication, along extrusion, comprises one of the main methods used to produce nanovesicles and help coating with nanoparticle cores. A marked decrease in ZP was observed for the BxPC3 nanovesicles (PCCM) and modified system PCCM@M when compared to Soluplus®/VES-GEM micelles (0.75/1) (M), showing the formation of negatively charged structures (**Figure S8 A-C**). It seems ultrasonication allows the preparation of BxPC3 nanovesicles (PCCM) with size ~ 200 nm, as reported in literature, surface charge < −10 mV, and low PDI (<0.2). Spherical structures in **Figure S8 D** corresponded to Soluplus®/VES-GEM micelles, distinct from structures resembling nanovesicles seen in **Figure S8 E**. However, it is not clear whether **Figure S8 F** corresponded to modified micelles, or just a mixture of nanovesicles and Soluplus®/VES-GEM micelles and if Soluplus®/VES-GEM micelles suffered alterations whether chemically or structurally. Nevertheless, TEM picture of the mixture of Soluplus®/VES-GEM micelles and BxPC3 membrane fragments after ultrasonication (**Figure S8 G**) showed a core–shell structure illusive of a membrane coating.

3.6. Cell membrane extraction through mild centrifugation, and preparation and characterization of BxPC3 cell membrane-modified Soluplus®/VES-GEM micelles

It is possible that working at 1 mg/mL concentration of Soluplus® (dilution of 30 times in PBS:water) may not be recommended, as may not correspond to the original concentrated Soluplus®/VES-GEM micelles formulation, according to the dynamic properties of micelles. Moreover, the high MW of Soluplus® may interfere on establishing the polymer-to-membrane ratio, as majority of polymers used for micelle preparation have considerably smaller MW. Hence, dilution was corrected to only 5 times (1:4 dilution of Soluplus®/VES-GEM micelles in water) and the medium used for preparing the micelles, nanovesicles and dilutions was corrected to only water. It is also possible the extraction procedure of membrane material may be too strong and yield small pieces of membrane which may hamper the procedure of nanovesicle obtainment and further coating. Hence, a distinct membrane extraction method was pursued, recurring to lower centrifugation speeds to preserve bigger membrane fragments and aid in the coating process (Liu et al., 2022; Zhou et al., 2024; Zou et al., 2023). Regarding extraction procedure, cell pellet was collected (**Figure S9 A**), subjected to hypotonic lysis (**Figure S9 B**), the mixture was ultrasonicated (**Figure S9 C**), centrifuged at 3200*g*/5 min/4 °C (**Figure S9 D**), supernatant collected at 7000*g*/10 min/4 °C, and the supernatant centrifuged at 15,000*g*/60 min/4 °C, obtaining membrane pellet at the bottom of the tube (**Figure S9 E**). As control procedure, protein (**Figure S9 F)** and DNA (**Figure S9 G**) content was quantified regularly, such as in the pellet and supernatant resulting from 3200*g* centrifugation, the supernatant after 15,000*g* centrifugation and the final membrane pellet resuspended in PBS (0.5 mL).

As expected, protein content decreased throughout the extraction procedure, as intracellular content and organelles were eliminated, and the small amount of protein content < 200 ng/mL may correspond to the protein content of purified membrane fragments. DNA content was expected to decrease due to nuclear material elimination, which decreased to < 100 ng/mL in the final pellet suspension in PBS (concentration of protein of 2.32 mg/mL). An attempt at assembling BxPC3 cell membrane-modified Soluplus®/VES-GEM micelles was made by co-extruding micelle cores (size ~ 90 nm, PDI ~ 0.35, ZP ~ −2 mV) with previously obtained BxPC3 nanovesicles (size ~ 150 nm, PDI ~ 0.1, ZP ~ −35 mV) (Fig. 5 **A-C**).

The BxPC3 membrane protein-to-polymer ratio was 30:1, not 1:1 to compensate large MW of Soluplus® and enable working conditions under mild dilution conditions. TEM pictures showed spherical structures for Soluplus®/VES-GEM micelles 1:4 dilution (Fig. 5 **D-F**) and 1:19 dilution (Fig. 5 **G-I**), which confirmed that the micelles can withstand significant dilution according to previous results and to the low CMC, and after extrusion procedure (Fig. 5 **J-L**) and nanovesicles (M−O). However, the coating was not evident in BxPC3 nanovesicle-modified Soluplus®/VES-GEM group (Fig. 5 **P-R**), which suggests Soluplus®/VES-GEM micelles due to the hydrophilic shell may not be prone to coating with cell membrane. When analysing DLS results, ZP of BxPC3 nanovesicle-modified Soluplus®/VES-GEM group increased to ~ −10 mV, which would not be expected if a coating was successful. When comparing to control BxPC3 nanovesicle and Soluplus®/VES-GEM micelles mixture, both size, PDI and surface charge remained very similar, which may additionally indicate that a coating was not achieved; only a mixture of micelles and nanovesicles.

Furthermore, these results mirror the challenge concerning the yield of membrane extraction procedure, which allowed obtainment of extremely low amounts of membrane material which limited the overall coating procedure optimization and forced the use of small concentrations of polymer in micelles. Nevertheless, BxPC3 nanovesicles with low PDI and well-defined size and structure could be obtained and may serve as suitable delivery systems for VES-GEM and other drugs in further studies. TEM pictures resulting from uranyl acetate staining also revealed well-defined spherical structures in the Soluplus®/VES-GEM group (**Figure S10 A-C**), relative monodisperse group of BxPC3 nanovesicles ~ 200 nm (**Figure S10 D-F**) and nanovesicles in the BxPC3 nanovesicle-modified Soluplus®/VES-GEM group **(Figure S10 G-I)** and in the control that was a physical mixture of micelles and BxPC3 nanovesicles (**Figure S10 J-K**).

Membrane coating optimization was further explored by testing additional polymer-to-membrane protein ratios (15:1, 6:1 and 3:1) enabling to increase the amount of membrane material used for preparation of the modified micelles. As the amount of membrane material increased, the size of the system increased slightly, which may be attributed to the existence of more BxPC3 nanovesicles, also accompanied by an increase in PDI, due to co-existence of two distinct particle systems (**Figure S11 A, B**). The ZP values were maintained > −15 mV regardless of amount of membrane material employed (**Figure S11 C**).

A decrease in surface charge was expected to occur as the amount of membrane material was increased, yielding superior quantity of nanovesicles prone to coat micelle cores and significantly lower polymer-to-conjugate ratios (**Figure S11 D, E**). Even for protein contents of 10 times the ones initially tested, the coating of single micelle was not evident. Alternatively, instead one micelle core being coated with a nanovesicle, the nanovesicle could encapsulate several micelles, as suggested by our results, showing structures with the same size of the nanovesicles and same ZP values of those shown by the BxPC3 nanovesicles. Hence, it is possible that either a mixture of micelle cores co-exists with BxPC3 nanovesicles, or the micelle cores (composed of amphiphilic copolymer Soluplus®) intercalate with the BxPC3 nanovesicles rendering PEGylated BxPC3 nanovesicles with poly(vinyl)-poly(caprolactam) hydrophobic segment intercalated in the hydrophobic compartment of the lipid membrane. TEM pictures of each formulation resulting from the titration procedure are shown in **Figure S12** and elicit the presence of nanovesicles, but the extent to which our methods were able to produce BxPC3 cell membrane-modified Soluplus®/VES-GEM micelles is not conclusive.

As doubts remained on the suitability of Soluplus®/VES-GEM micelles to be coated with BxPC3 cell membrane, according to DLS and TEM results, a parallel experiment was set up to verify the adequateness of the experimental procedure by using PLGA rigid nanoparticles as control cores widely explored in literature. PLGA nanoparticles were obtained with low PDI (<0.1) and sized ~ 100 nm with strong negative surface charge (~−40 mV) (**Figure S13 A-C**) and showing a spherical morphology (**Figure S13 E-G**). A coating procedure similar to the previously described above was conducted using a polymer:protein 1:1 w/w ratio (**Figure S13 D**) The ZP value of the modified system, PLGA@M (~–33 mV), approximated to the one found for the BxPC3 cell membranes, M (~−29 mV), but the strong negative charge obtained for PLGA nanoparticles, either extruded or non-extruded (<−30 mV) may influence these results (**Figure S13 C**). Extrusion increased the polydispersity and size of the PLGA population (**Figure S13 A-C, H-J**). BxPC3 nanovesicles were obtained as explained above (**Figure S13 K-M**) and used for the coating procedure. TEM pictures showed the presence of a thin non-continuous coating layer around PLGA cores (**Figure S13 N-P**), which was not evident in the control mixture of BxPC3 nanovesicles with PLGA cores, non-modified **(Figure S13 Q-S).** Regarding size of the obtained modified PLGA cores, PLGA@M, it would be expected to have an increase in size of about ~ 15 nm which corresponds to the average width of the lipid bilayer, and the final size of PLGA@M system was similar to the nanovesicles, M, group (~150 nm). Although DLS results are not conclusive and further characterization techniques are warranted, these findings clearly indicated that PLGA nanoparticles are more prone to be coated when compared to micelles.

The possible presence of a thin cell membrane coating on the surface of Soluplus® micelles was further analysed through CLSM as reported (Duan et al., 2022; Chen et al., 2023). The blank micelles were loaded with Nile red and the membrane nanovesicles labelled with DOPE-Atto 488 dye. CLSM picture showed only spherical structures with green

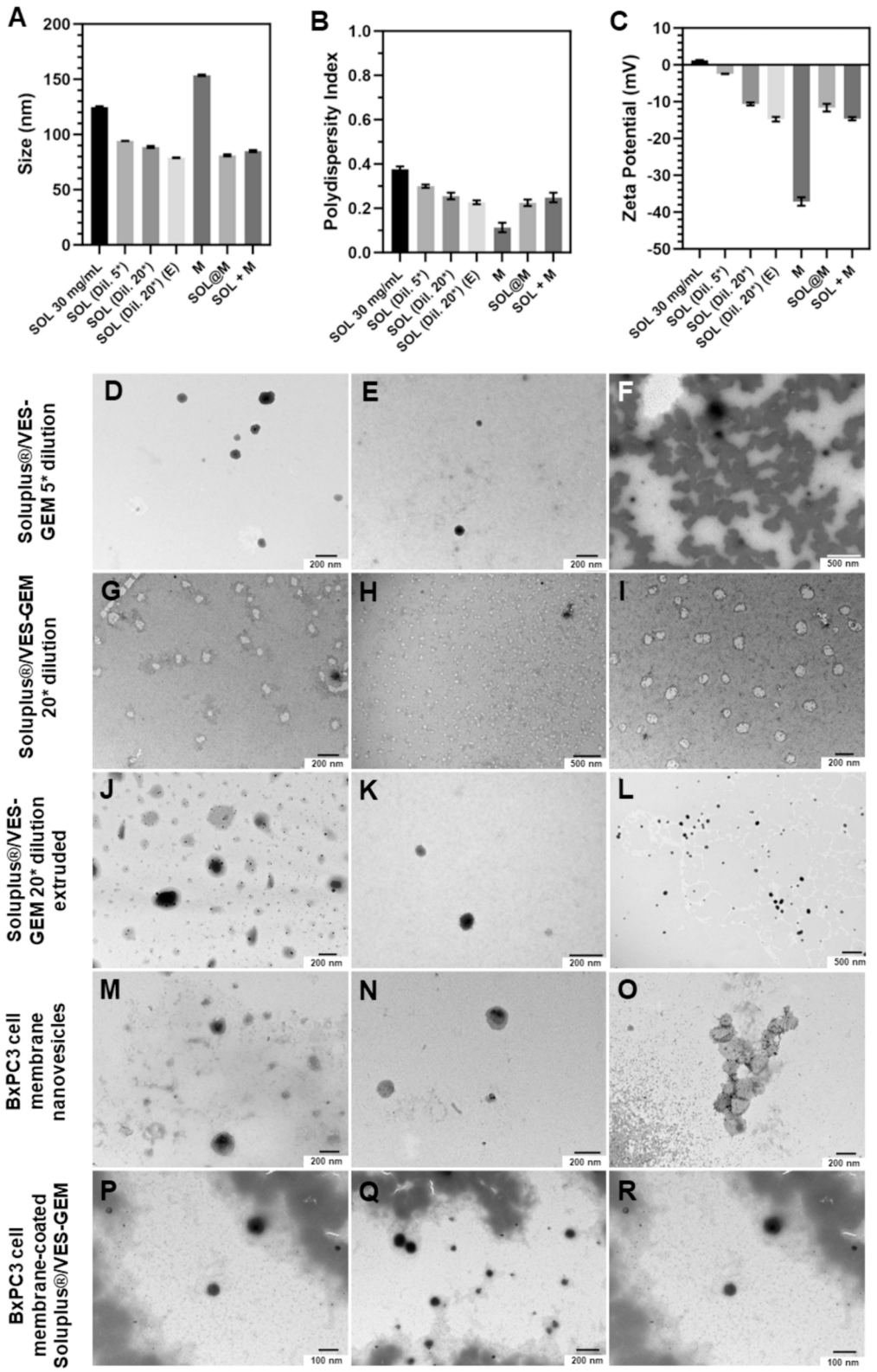

Fig. 5. Size (A), PDI (B) and ZP (C) of non-filtered Soluplus®/VES-GEM micelles (polymer concentration of 29.8 mg/mL), Soluplus®/VES-GEM micelles 1:4 dilution in water (polymer concentration of 6 mg/mL), Soluplus®/VES-GEM micelles final dilution compensating volume added containing BxPC3 nanovesicles and DLS dilution measurement 1:1 in water (polymer concentration of 1.2 mg/mL) and extruded counterparts, BxPC3 nanovesicles, BxPC3 nanovesicle-modified Soluplus®/VES-GEM micelles (polymer-to-protein ratio of 30:1) and mixture of extruded Soluplus®/VES-GEM micelles 1:4 dilution in water with BxPC3 nanovesicles and diluted for DLS measurement, as second control, and under same polymer-to-protein membrane ratio. TEM pictures of the Soluplus®/VES-GEM micelles 1:4 dilution in water (polymer concentration of 6 mg/mL) (D-F), final dilution (1:19) (G-I) and final dilution (1:19) after extrusion (J-L), BxPC3 nanovesicles (M−O) and BxPC3 nanovesicle-modified Soluplus®/VES-GEM micelles (polymer-to-protein ratio of 6:1) (P-R). Three photos were taken independently from the same prepared sample for each formulation. The samples were not filtered. Samples were stained with phosphotungstic acid 2 %.

color, sized 150 nm, which correspond to the BxPC3 nanovesicles. No signal regarding micelle cores (red) was detected (**Figure S14**). This may be explained by the low encapsulation of Nile red in Soluplus® micelles and, more interestingly, by the possibility of intercalation of Soluplus® within the lipid bilayer of BxPC3 nanovesicles, disintegration of micelle structure and release of hydrophobic Nile red, explaining the absence of signal. Other techniques with higher resolution may help elucidating this issue in the future (Wu et al., 2024).

4. Conclusion

In this work, the hydrophilic gemcitabine (GEM) was encapsulated as a lipophilic conjugate with vitamin E succinate (VES-GEM) in Soluplus® micelles, forming Soluplus®/VES-GEM micelles. This prodrug approach facilitated encapsulation of the anticancer drug into the self-assembled copolymer micelles. Soluplus®/VES-GEM micelles bearing an optimal polymer-to-conjugate ratio of 0.75/1 were prepared through the solvent evaporation method and showed size < 100 nm, PDI < 0.4 and slightly negative surface charge, as well as good encapsulation efficiency (~80 %) and excellent stability. Soluplus®/VES-GEM micelles caused negligible hemolytic activity but exhibited significant cytotoxic activity in BxPC3 pancreatic cancer (PC) cells, namely ~25 % cell viability attained for 100 μM VES-GEM concentration, and comparable to that of free GEM control. Therefore, although *in vitro* drug release was negligible at both pH 7.4 and 5.0 under the tested conditions, significant cytotoxicity observed in BxPC3 cell line studies confirms that the VES-GEM formulation can be internalized and release GEM effectively within cells. The targeting efficacy was not extensively studied, but previous studies suggested that homotypic targeting mechanisms, along with the EPR effect, prolonged circulation, immune evasion, and enhanced cellular uptake, could collectively facilitate efficient systemic circulation and targeted delivery of the drug. Thus, Soluplus®/VES-GEM micelles were explored as suitable cores for biomimetic coating with BxPC3 cell membrane. BxPC3 cell membrane nanovesicles were successfully produced with low PDI, size ~ 150 nm and with a noticeable spherical structure, with ZP typical of cell membranes (<-30 mV). BxPC3 cell membrane-modified Soluplus®/VES-GEM system displayed size ~ 75 nm, and significative reduction in ZP to ~ −14 mV when compared to non-modified Soluplus®/VES-GEM micelles (~−2 mV). However, there is a need for further improvement of characterization techniques that allowed verification of the extent of the coating. Our study demonstrated that DLS, TEM and CLSM techniques are not very suitable for confirming the coating of soft, hydrophilic micelles with cell membranes due to the limitations of the techniques to distinguish between coated and non-coated micelles. Further *in vivo* studies will be needed to validate the targeting mechanisms and optimize the therapeutic efficacy of the VES-GEM formulation.

Funding

This work received financial support from grant FCT SFRH/BD/148771/2019 by the Fundação para a Ciência e Tecnologia (FCT, Portugal). The work was also partially supported by the Ministerio de Ciencia e Innovación MCIN/AEI/10.13039/501100011033 [PID2023-150422OB-I00] (Spain) and FEDER.

CRediT authorship contribution statement

Miguel Pereira-Silva: Writing – review & editing, Writing – original draft, Visualization, Validation, Software, Methodology, Investigation, Formal analysis, Conceptualization. **Luis Diaz-Gomez:** Writing – review & editing, Writing – original draft, Visualization, Software, Methodology, Investigation, Formal analysis. **Bárbara Blanco-Fernandez:** Writing – review & editing, Writing – original draft, Visualization, Validation, Software, Methodology, Investigation, Data curation. **Alba Ferreirós:** Validation, Supervision, Resources, Methodology, Investigation. **Francisco Veiga:** Writing – review & editing, Supervision, Project administration, Funding acquisition, Conceptualization. **Angel Concheiro:** Writing – review & editing, Supervision, Resources, Project administration, Funding acquisition, Conceptualization. **Ana Cláudia Paiva-Santos:** Writing – review & editing, Supervision, Software, Resources, Project administration, Funding acquisition, Conceptualization. **Carmen Alvarez-Lorenzo:** Writing – review & editing, Writing – original draft, Supervision, Resources, Project administration, Investigation, Funding acquisition, Formal analysis, Conceptualization.

Declaration of competing interest

The authors declare that they have no known competing financial interests or personal relationships that could have appeared to influence the work reported in this paper.

Data availability

The authors confirm that the data supporting the findings of this study are available within the article and its supplementary material. Additional data supporting the findings of this study are available from the corresponding author upon reasonable request.

Acknowledgements

The authors would like to thank M. Vivero-Lopez for help with HPLC methodology and M. Pita-Vilar for help with the cell culture experiments. B.B.-F. acknowledges a Ramón y Cajal contract [RYC2022-037421-I]

Appendix A. Supplementary material

Supplementary data to this article can be found online at https://doi.org/10.1016/j.ijpharm.2024.124529.

References

Abouelmagd, S.A., Sun, B., Chang, A.C., Ku, Y.J., Yeo, Y., 2015. Release kinetics study of poorly water-soluble drugs from nanoparticles: are we doing it right? Mol. Pharm. 12 (3), 997–1003. https://doi.org/10.1021/mp500817h.

Alambiaga-Caravaca, A.M., Calatayud-Pascual, M.A., Rodilla, V., Concheiro, A., Lopez-Castellano, A., Alvarez-Lorenzo, C., 2020. Micelles of progesterone for topical eye administration: interspecies and intertissues differences in ex vivo ocular permeability. Pharmaceutics 12 (8), 702. https://doi.org/10.3390/pharmaceutics12080702.

Alopaeus, J.F., Hagesaether, E., Tho, I., 2019. Micellisation mechanism and behaviour of soluplus(R)(-)furosemide micelles: preformulation studies of an oral nanocarrier-based system. Pharmaceuticals (Basel) 12 (1), 15. https://doi.org/10.3390/ph12010015.

Attia, M.S., Elshahat, A., Hamdy, A., Fathi, A.M., Emad-Eldin, M., Ghazy, F.-E.-S., Chopra, H., Ibrahim, T.M., 2023. Soluplus® as a solubilizing excipient for poorly water-soluble drugs: recent advances in formulation strategies and pharmaceutical product features. J. Drug. Deliv. Sci. Technol. 84 (104519) https://doi.org/10.1016/j.jddst.2023.104519.

Basha, M., Salama, A., Noshi, S.H., 2020. Soluplus((R)) based solid dispersion as fast disintegrating tablets: a combined experimental approach for enhancing the dissolution and antiulcer efficacy of famotidine. Drug Dev. Ind. Pharm., 46(2), 253–263, doi: 10.1080/03639045.2020.1716376.

Bernabeu, E., Gonzalez, L., Cagel, M., Gergic, E.P., Moretton, M.A., Chiappetta, D.A., 2016. Novel Soluplus((R))-TPGS mixed micelles for encapsulation of paclitaxel with enhanced in vitro cytotoxicity on breast and ovarian cancer cell lines. Colloids Surf. B Biointerfaces 140 (403–411). https://doi.org/10.1016/j.colsurfb.2016.01.003.

Bildstein, L., Dubernet, C., Couvreur, P., 2011. Prodrug-based intracellular delivery of anticancer agents. Adv. Drug Deliv. Rev. 63 (1–2), 3–23. https://doi.org/10.1016/j.addr.2010.12.005.

Blanco-Fernandez, B., Rey-Vinolas, S., Bagci, G., Rubi-Sans, G., Otero, J., Navajas, D., Perez-Amodio, S., Engel, E., 2022. Bioprinting decellularized breast tissue for the development of three-dimensional breast cancer models. ACS Appl. Mater. Interfaces 14 (26), 29467–29482. https://doi.org/10.1021/acsami.2c00920.

Bonde, G.V., Ajmal, G., Yadav, S.K., Mittal, P., Singh, J., Bakde, B.V., Mishra, B., 2020. Assessing the viability of Soluplus(R) self-assembled nanocolloids for sustained delivery of highly hydrophobic lapatinib (anticancer agent): Optimisation and in-vitro characterisation. Colloids Surf. B Biointerfaces 185 (110611). https://doi.org/10.1016/j.colsurfb.2019.110611.

Bulanadi, J.C., Xue, A., Gong, X., Bean, P.A., Julovi, S.M., de Campo, L., Smith, R.C., Moghaddam, M.J., 2020. Biomimetic gemcitabine-lipid prodrug nanoparticles for pancreatic cancer. ChemPlusChem 85 (6), 1283–1291. https://doi.org/10.1002/cplu.202000253.

Cao, H., Jiang, B., Yang, Y., Zhao, M., Sun, N., Xia, J., Gao, X., Li, J., 2021. Cell membrane covered polydopamine nanoparticles with two-photon absorption for precise photothermal therapy of cancer. J. Colloid Interface Sci. 604 (596–603) https://doi.org/10.1016/j.jcis.2021.07.004.

Ch, S., Padaga, S.G., Ghosh, B., Roy, S., Biswas, S., 2023. Chitosan-poly(lactide-co-glycolide)/poloxamer mixed micelles as a mucoadhesive thermo-responsive moxifloxacin eye drop to improve treatment efficacy in bacterial keratitis. Carbohydr. Polym. 312 (120822) https://doi.org/10.1016/j.carbpol.2023.120822.

Chen, H., Pu, W., Hu, X., Yang, C., Zhao, G., Hu, H., Zhang, J., 2023. Rational engineering of a mitochondrial-mimetic therapy for targeted treatment of dilated cardiomyopathy by precisely regulating mitochondrial homeostasis. Adv. Funct. Mat. 33 (49) https://doi.org/10.1002/adfm.202301918.

Daman, Z., Ostad, S., Amini, M., Gilani, K., 2014. Preparation, optimization and in vitro characterization of stearoyl-gemcitabine polymeric micelles: a comparison with its self-assembled nanoparticles. Int. J. Pharm. 468 (1–2), 142–151. https://doi.org/10.1016/j.ijpharm.2014.04.021.

Di, Y., Gao, Y., Gai, X., Wang, D., Wang, Y., Yang, X., Zhang, D., Pan, W., Yang, X., 2017. Co-delivery of hydrophilic gemcitabine and hydrophobic paclitaxel into novel polymeric micelles for cancer treatment. RSC Adv. 7 (39), 24030–24039. https://doi.org/10.1039/C7RA02909H.

Dian, L., Yu, E., Chen, X., Wen, X., Zhang, Z., Qin, L., Wang, Q., Li, G., Wu, C., 2014. Enhancing oral bioavailability of quercetin using novel soluplus polymeric micelles. Nanoscale Res. Lett. 9 (1), 2406. https://doi.org/10.1186/1556-276X-9-684.

Ding, Y., Wang, C., Wang, Y., Xu, Y., Zhao, J., Gao, M., Ding, Y., Peng, J., Li, L., 2018. Development and evaluation of a novel drug delivery: Soluplus((R))/TPGS mixed micelles loaded with piperine in vitro and in vivo. Drug Dev. Ind. Pharm, 44(9), 1409-1416, doi: 10.1080/03639045.2018.1472277.

Ding, Y., Ding, Y., Wang, Y., Wang, C., Gao, M., Xu, Y., Ma, X., Wu, J., Li, L., 2020. Soluplus((R))/TPGS mixed micelles for co-delivery of docetaxel and piperine for combination cancer therapy. Pharm. Dev. Technol, 25(1), 107–115, doi: 10.1080/10837450.2019.1679834.

Dong, K., Zhang, M., Liu, Y., Gao, X., Wu, X., Shi, D., Guo, C., Wang, J., 2023. Pterostilbene-loaded soluplus/poloxamer 188 mixed micelles for protection against acetaminophen-induced acute liver injury. Mol. Pharm. 20 (2), 1189–1201. https://doi.org/10.1021/acs.molpharmaceut.2c00881.

Duan, R., Sun, K., Fang, F., Wang, N., He, R., Gao, Y., Jing, L., Li, Y., Gong, Z., Yao, Y., Luan, T., Zhang, C., Zhang, J., Zhao, Y., Xie, H., Zhou, Y., Teng, J., Zhang, J., Jia, Y., 2022. An ischemia-homing bioengineered nano-scavenger for specifically alleviating multiple pathogeneses in ischemic stroke. J. Nanobiotechnol. 20 (1), 397. https://doi.org/10.1186/s12951-022-01602-7.

Emamzadeh, M., Desmaele, D., Couvreur, P., Pasparakis, G., 2018. Dual controlled delivery of squalenoyl-gemcitabine and paclitaxel using thermo-responsive polymeric micelles for pancreatic cancer. J. Mater. Chem. B 6 (15), 2230–2239. https://doi.org/10.1039/c7tb02899g.

Fang, Y., Du, F., Xu, Y., Meng, H., Huang, J., Zhang, X., Lu, W., Liu, S., Yu, J., 2015. Enhanced cellular uptake and intracellular drug controlled release of VESylated gemcitabine prodrug nanocapsules. Colloids Surf. B Biointerfaces 128 (357–362). https://doi.org/10.1016/j.colsurfb.2015.02.028.

Fang, R.H., Hu, C.M., Luk, B.T., Gao, W., Copp, J.A., Tai, Y., O'Connor, D.E., Zhang, L., 2014. Cancer cell membrane-coated nanoparticles for anticancer vaccination and drug delivery. Nano Lett. 14 (4), 2181–2188. https://doi.org/10.1021/nl500618u.

Feng, X., Chen, Y., Li, L., Zhang, Y., Zhang, L., Zhang, Z., 2020. Preparation, evaluation and metabolites study in rats of novel amentoflavone-loaded TPGS/soluplus mixed nanomicelles. Drug Deliv, 27(1), 137–150 doi: 10.1080/10717544.2019.1709920.

Gaudin, A., Song, E., King, A.R., Saucier-Sawyer, J.K., Bindra, R., Desmaele, D., Couvreur, P., Saltzman, W.M., 2016. PEGylated squalenoyl-gemcitabine nanoparticles for the treatment of glioblastoma. Biomaterials 105 (136–144). https://doi.org/10.1016/j.biomaterials.2016.07.037.

Ghosh, B., Biswas, S., 2021. Polymeric micelles in cancer therapy: State of the art. J. Control. Release 332 (127–147). https://doi.org/10.1016/j.jconrel.2021.02.016.

Grimaudo, M.A., Pescina, S., Padula, C., Santi, P., Concheiro, A., Alvarez-Lorenzo, C., Nicoli, S., 2018. Poloxamer 407/TPGS mixed micelles as promising carriers for cyclosporine ocular delivery. Mol. Pharm. 15 (2), 571–584. https://doi.org/10.1021/acs.molpharmaceut.7b00939.

Guo, R., Long, Y., Lu, Z., Deng, M., He, P., Li, M., He, Q., 2020. Enhanced stability and efficacy of GEM-TOS prodrug by co-assembly with antimetastatic shell LMWH-TOS. Acta Pharm. Sin. B 10 (10), 1977–1988. https://doi.org/10.1016/j.apsb.2019.06.008.

Han, H., Li, S., Zhong, Y., Huang, Y., Wang, K., Jin, Q., Ji, J., Yao, K., 2022. Emerging pro-drug and nano-drug strategies for gemcitabine-based cancer therapy. Asian J. Pharm. Sci. 17 (1), 35–52. https://doi.org/10.1016/j.ajps.2021.06.001.

He, L., Zhao, J., Li, H., Xie, B., Xu, L., Huang, G., Liu, T., Gu, Z., Chen, T., 2023. Metabolic reprogramming of NK cells by black phosphorus quantum dots potentiates cancer immunotherapy. Adv Sci (weinh) 10 (8). https://doi.org/10.1002/advs.202202519.

Holland, J., Castrejon-Pita, A.A., Tuinier, R., Aarts, D., Nott, T.J., 2023. Surface tension measurement and calculation of model biomolecular condensates. Soft Matter 19 (45), 8706–8716. https://doi.org/10.1039/d3sm00820g.

Huang, X., Mu, N., Ding, Y., Huang, R., Wu, W., Li, L., Chen, T., 2024. Tumor microenvironment targeting for glioblastoma multiforme treatment via hybrid cell membrane coating supramolecular micelles. J. Control. Release 366 (194–203). https://doi.org/10.1016/j.jconrel.2023.12.033.

Jeon, S.I., Yang, S., Shim, M.K., Kim, K., 2022. Cathepsin B-responsive prodrugs for cancer-targeted therapy: Recent advances and progress for clinical translation. Nano Res. 15 (8), 7247–7266. https://doi.org/10.1007/s12274-022-4354-y.

Jiang, S., Mou, Y., He, H., Yang, D., Qin, L., Zhang, F., Zhang, P., 2019. Preparation and evaluation of self-assembly Soluplus((R))-sodium cholate-phospholipid ternary mixed micelles of docetaxel. Drug Dev Ind Pharm, 45(11), 1788–1798, doi: 10.1080/03639045.2019.1660365.

Jin, I.S., Jo, M.J., Park, C.W., Chung, Y.B., Kim, J.S., Shin, D.H., 2020. Physicochemical, pharmacokinetic, and toxicity evaluation of soluplus((R)) polymeric micelles encapsulating fenbendazole. Pharmaceutics 12 (10), 1000. https://doi.org/10.3390/pharmaceutics12101000.

Jin, R., Zhang, G., Tang, L., Li, M., Yang, M., Li, J., Wang, Z., Guan, F., 2024. Active-targeting biomimetic polymer nanoparticles for NIR fluorescence imaging and enhanced chemo-sonodynamic therapy of cancer. ACS Appl.Nano Mater. 7 (4), 3968–3976. https://doi.org/10.1021/acsanm.3c05575.

Jin, X., Zhou, B., Xue, L., San, W., 2015. Soluplus((R)) micelles as a potential drug delivery system for reversal of resistant tumor. Biomed. Pharmacother. 69 (388–95) https://doi.org/10.1016/j.biopha.2014.12.028.

Kakwere, H., Ingham, E.S., Tumbale, S.K., Ferrara, K.W., 2020. Gemcitabine-retinoid prodrug loaded nanoparticles display in vitro antitumor efficacy towards drug-resilient human PANC-1 pancreatic cancer cells. Mater Sci Eng C Mater Biol Appl. 117, 111251 https://doi.org/10.1016/j.msec.2020.111251.

Khare, V., Sakarchi, W.A., Gupta, P.N., Curtis, A.D.M., Hoskins, C., 2016. Synthesis and characterization of TPGS–gemcitabine prodrug micelles for pancreatic cancer therapy. RSC Adv. 6 (65), 60126–60137. https://doi.org/10.1039/C6RA09347G.

Kirstein, M.N., Hassan, I., Guire, D.E., Weller, D.R., Dagit, J.W., Fisher, J.E., Remmel, R. P., 2006. High-performance liquid chromatographic method for the determination of gemcitabine and 2',2'-difluorodeoxyuridine in plasma and tissue culture media. J. Chromatogr. B Anal. Technol. Biomed. Life Sci. 835 (1–2), 136–142. https://doi.org/10.1016/j.jchromb.2006.03.023.

Li, S., Jiang, W., Yuan, Y., Sui, M., Yang, Y., Huang, L., Jiang, L., Liu, M., Chen, S., Zhou, X., 2020a. Delicately designed cancer cell membrane-camouflaged nanoparticles for targeted (19)F MR/PA/FL imaging-guided photothermal therapy. ACS Appl. Mater. Interfaces 12 (51), 57290–57301. https://doi.org/10.1021/acsami.0c13865.

Li, Y., Mei, T., Han, S., Han, T., Sun, Y., Zhang, H., An, F., 2020b. Cathepsin B-responsive nanodrug delivery systems for precise diagnosis and targeted therapy of malignant tumors. Chin. Chem. Lett. 31 (12), 3027–3040. https://doi.org/10.1016/j.cclet.2020.05.027.

Li, J., Wu, Y., Wang, J., Xu, X., Zhang, A., Li, Y., Zhang, Z., 2023. Macrophage membrane-coated nano-gemcitabine promotes lymphocyte infiltration and synergizes AntiPD-L1 to restore the tumoricidal function. ACS Nano 17 (1), 322–336. https://doi.org/10.1021/acsnano.2c07861.

Lim, C., Hwang, D., Yazdimamaghani, M., Atkins, H.M., Hyun, H., Shin, Y., Ramsey, J.D., Radler, P.D., Mott, K.R., Perou, C.M., Sokolsky-Papkov, M., Kabanov, A.V., 2023. High-dose paclitaxel and its combination with CSF1R inhibitor in polymeric micelles for chemoimmunotherapy of triple negative breast cancer. Nano Today 51 (101884). https://doi.org/10.1016/j.nantod.2023.101884.

Liu, L., Yu, W., Seitsonen, J., Xu, W., Lehto, V.P., 2022b. Correct identification of the core-shell structure of cell membrane-coated polymeric nanoparticles. Chemistry 28 (68), e202200947.

Liu, F., Zhou, Y., Liu, L., Pan, H., Liu, H., 2022a. Effect of 2-ethylbutyric acid on thermodynamics stability of various nonionic surfactants tanshione-loaded micelles. J. Mol. Liq. 362 (119775) https://doi.org/10.1016/j.molliq.2022.119775.

Longati, P., Jia, X., Eimer, J., Wagman, A., Witt, M.R., Rehnmark, S., Verbeke, C., Toftgard, R., Lohr, M., Heuchel, R.L., 2013. 3D pancreatic carcinoma spheroids induce a matrix-rich, chemoresistant phenotype offering a better model for drug testing. BMC Cancer 13 (95). https://doi.org/10.1186/1471-2407-13-95.

Lu, Y., Fan, L., Wang, J., Hu, M., Wei, B., Shi, P., Li, J., Feng, J., Zheng, Y., 2024. Cancer cell membrane-based materials for biomedical applications. Small 20 (7), e2306540.

Luo, Y., Wang, J., Xu, L., Du, Q., Fang, N., Wu, H., Liu, F., Hu, L., Xu, J., Hou, J., Zhong, Y., Liu, Y., Wang, Z., Ran, H., Guo, D., 2022. A theranostic metallodrug modulates immunovascular crosstalk to combat immunosuppressive liver cancer. Acta Biomater. 154 (478–496) https://doi.org/10.1016/j.actbio.2022.10.032.

Mahmud, M.M., Pandey, N., Winkles, J.A., Woodworth, G.F., Kim, A.J., 2024. Toward the scale-up production of polymeric nanotherapeutics for cancer clinical trials. Nano Today 56 (102314). https://doi.org/10.1016/j.nantod.2024.102314.

Malhotra, S., Dumoga, S., Joshi, A., Mohanty, S., Singh, N., 2021. Polymeric micelles coated with hybrid nanovesicles enhance the therapeutic potential of the reversible topoisomerase inhibitor camptothecin in a mouse model. Acta Biomater. 121 (579–591) https://doi.org/10.1016/j.actbio.2020.11.049.

Mao, X., Wu, S., Huang, D., Li, C., 2024. Complications and comorbidities associated with antineoplastic chemotherapy: Rethinking drug design and delivery for anticancer therapy. Acta Pharm. Sin. B 14, 2901–2926. https://doi.org/10.1016/j.apsb.2024.03.006.

Marques, S.S., Ramos II, S.R., Fernandes, L., Barreiros, S.A.C., Lima, S., Reis, M.R.M.D., Segundo, M.A., 2020. Insights on ultrafiltration-based separation for the purification and quantification of methotrexate in nanocarriers. Molecules 25 (8), 1879. https://doi.org/10.3390/molecules25081879.

Mateos, H., Gentile, L., Murgia, S., Colafemmina, G., Collu, M., Smets, J., Palazzo, G., 2022. Understanding the self-assembly of the polymeric drug solubilizer Soluplus®. J. Colloid Interface Sci. 611 (224–234) https://doi.org/10.1016/j.jcis.2021.12.016.

Norouzi, P., Amini, M., Dinarvand, R., Arefian, E., Seyedjafari, E., Atyabi, F., 2020. Co-delivery of gemcitabine prodrug along with anti NF-kappaB siRNA by tri-layer micelles can increase cytotoxicity, uptake and accumulation of the system in the

cancers. Mater. Sci. Eng. C Mater. Biol. Appl. 116 (111161) https://doi.org/10.1016/j.msec.2020.111161.
Pan, H., Yang, S., Gao, L., Zhou, J., Cheng, W., Chen, G., Shuhang, W., Li, N., Veranič, P., Musiol, R., Cai, Q., Shubhra, Q.T.H., 2024. At the crossroad of nanotechnology and cancer cell membrane coating: Expanding horizons with engineered nanoplatforms for advanced cancer therapy harnessing homologous tumor targeting. Coord. Chem. Rev. 506 (215712) https://doi.org/10.1016/j.ccr.2024.215712.
Pereira-Silva, M., Santos, A.C., Conde, J., Hoskins, C., Concheiro, A., Alvarez-Lorenzo, C., Veiga, F., 2020. Biomimetic cancer cell membrane-coated nanosystems as next-generation cancer therapies. Expert Opin Drug Deliv, 17(11), 1515–1518, doi: 10.1080/17425247.2020.1813109.
Pereira-Silva, M., Miranda-Pastoriza, D., Diaz-Gomez, L., Sotelo, E., Paiva-Santos, A.C., Veiga, F., Concheiro, A., Alvarez-Lorenzo, C., 2024. Gemcitabine-vitamin E prodrug-loaded micelles for pancreatic cancer therapy. Pharmaceutics 16 (1), 95. https://doi.org/10.3390/pharmaceutics16010095.
Piazzini, V., Vasarri, M., Degl'Innocenti, D., Guastini, A., Barletta, E., Salvatici, M.C., Bergonzi, M.C., 2019. Comparison of chitosan nanoparticles and soluplus micelles to optimize the bioactivity of posidonia oceanica extract on human neuroblastoma cell migration. Pharmaceutics 11 (12), 655. https://doi.org/10.3390/pharmaceutics11120655.
Pignatello, R., Corsaro, R., Bonaccorso, A., Zingale, E., Carbone, C., Musumeci, T., 2022. Soluplus((R)) polymeric nanomicelles improve solubility of BCS-class II drugs. Drug Deliv. Transl. Res. 12 (8), 1991–2006. https://doi.org/10.1007/s13346-022-01182-x.
Pote, M.S., Gacche, R.N., 2023. ATP-binding cassette efflux transporters and MDR in cancer. Drug Discov. Today 28 (5), 103537. https://doi.org/10.1016/j.drudis.2023.103537.
Pramanik, N., Gupta, A., Ghanwatkar, Y., Mahato, R.I., 2024. Recent advances in drug delivery and targeting for the treatment of pancreatic cancer. J. Control. Release 366 (231–260). https://doi.org/10.1016/j.jconrel.2023.12.053.
Quan, L., Zhang, Y., Crielaard, B.J., Dusad, A., Lele, S.M., Rijcken, C.J.F., Metselaar, J.M., Kostkova, H., Etrych, T., Ulbrich, K., Kiessling, F., Mikuls, T.R., Hennink, W.E., Storm, G., Lammers, T., Wang, D., 2014. Nanomedicines for inflammatory arthritis: head-to-head comparison of glucocorticoid-containing polymers, micelles, and liposomes. ACS Nano 8 (1), 458–466. https://doi.org/10.1021/nn4048205.
Rajan, N., Habermehl, J., Cote, M.F., Doillon, C.J., Mantovani, D., 2006. Preparation of ready-to-use, storable and reconstituted type I collagen from rat tail tendon for tissue engineering applications. Nat. Protoc. 1 (6), 2753–2758. https://doi.org/10.1038/nprot.2006.430.
Rao, M., Gaikwad, P., Misal, P., Gandhi, S.V., 2024. Phyto-cosmeceutical gel containing curcumin and quercetin loaded mixed micelles for improved anti-oxidant and photoprotective activity. Colloids Surf. B 237 (113837). https://doi.org/10.1016/j.colsurfb.2024.113837.
Raza, F., Evans, L., Motallebi, M., Zafar, H., Pereira-Silva, M., Saleem, K., Peixoto, D., Rahdar, A., Sharifi, E., Veiga, F., Hoskins, C., Paiva-Santos, A.C., 2023. Liposome-based diagnostic and therapeutic applications for pancreatic cancer. Acta Biomater. 157 (1–23) https://doi.org/10.1016/j.actbio.2022.12.013.
Riedel, J., Pibuel, M., Bernabeu, E., Poodts, D., Díaz, M., Allo, M., Parola, L., Hajos, S., Lázaro-Martínez, J.M., Salgueiro, M.J., Santander, Y., Lompardía, S., Moretton, M. A., Höcht, C., Chiappetta, D.A., 2022. Glycosylated paclitaxel mixed nanomicelles: Increasing drug brain accumulation and enhancing its in vitro antitumoral activity in glioblastoma cell lines. J. Drug Deliv. Sci. Technol. 68 (103046) https://doi.org/10.1016/j.jddst.2021.103046.
Rodriguez-Evora, M., Reyes, R., Alvarez-Lorenzo, C., Concheiro, A., Delgado, A., Evora, C., 2014. Bone regeneration induced by an in situ gel-forming poloxamine, bone morphogenetic protein-2 system. J. Biomed. Nanotechnol. 10 (6), 959–969. https://doi.org/10.1166/jbn.2014.1801.
Rouco, H., Garcia-Garcia, P., Evora, C., Diaz-Rodriguez, P., Delgado, A., 2022. Screening strategies for surface modification of lipid-polymer hybrid nanoparticles. Int. J. Pharm. 624 (121973) https://doi.org/10.1016/j.ijpharm.2022.121973.
Ruiz, E., Orozco, V.H., Hoyos, L.M., Giraldo, L.F., 2024. Quantification of pluronic F127 used on PLGA nanoparticle preparation and comparing purification techniques by centrifugation, tangential flow filtration, and ultrafiltration. Eur. Polym. J. 208 (112887) https://doi.org/10.1016/j.eurpolymj.2024.112887.
Shields, M.A., Dangi-Garimella, S., Redig, A.J., Munshi, H.G., 2012. Biochemical role of the collagen-rich tumour microenvironment in pancreatic cancer progression. Biochem. J. 441 (2), 541–552. https://doi.org/10.1042/BJ20111240.
Siegel, R.L., Giaquinto, A.N., Jemal, A., 2024. Cancer statistics, 2024. CA Cancer J. Clin. 74 (1), 12–49. https://doi.org/10.3322/caac.21820.
Singh, J., Mittal, P., Vasant Bonde, G., Ajmal, G., Mishra, B., 2018. Design, optimization, characterization and in-vivo evaluation of Quercetin enveloped Soluplus(R)/P407 micelles in diabetes treatment. Artif Cells Nanomed. Biotechnol., 46(sup3), S546-S555, doi: 10.1080/21691401.2018.1501379.
Soprano, E., Alvarez, A., Pelaz, B., Del Pino, P., Polo, E., 2020. Plasmonic cell-derived nanocomposites for light-controlled cargo release inside living cells. Adv. Biosyst. 4 (3) https://doi.org/10.1002/adbi.201900260.
Sun, J., Chen, Y., Xu, J., Song, X., Wan, Z., Du, Y., Ma, W., Li, X., Zhang, L., Li, S., 2020. High loading of hydrophobic and hydrophilic agents via small immunostimulatory carrier for enhanced tumor penetration and combinational therapy. Theranostics 10 (3), 1136–1150. https://doi.org/10.7150/thno.38287.
Tarannum, M., Vivero-Escoto, J.L., 2022. Nanoparticle-based therapeutic strategies targeting major clinical challenges in pancreatic cancer treatment. Adv. Drug Deliv. Rev. 187 (114357) https://doi.org/10.1016/j.addr.2022.114357.
Tehrani, S.F., Bharadwaj, P., Leblond Chain, J., Roullin, V.G., 2023. Purification processes of polymeric nanoparticles: How to improve their clinical translation? J. Control. Release 360 (591–612). https://doi.org/10.1016/j.jconrel.2023.06.038.
Twal, S., Jaber, N., Al-Remawi, M., Hamad, I., Al-Akayleh, F., Alshaer, W., 2024. Dual stimuli-responsive polymeric nanoparticles combining soluplus and chitosan for enhanced breast cancer targeting. RSC Adv. 14 (5), 3070–3084. https://doi.org/10.1039/d3ra08074a.
Varela-Garcia, A., Concheiro, A., Alvarez-Lorenzo, C., 2018. Soluplus micelles for acyclovir ocular delivery: Formulation and cornea and sclera permeability. Int. J. Pharm. 552 (1–2), 39–47. https://doi.org/10.1016/j.ijpharm.2018.09.053.
Vivero-Lopez, M., Sparacino, C., Quelle-Regaldie, A., Sanchez, L., Candal, E., Barreiro-Iglesias, A., Huete-Toral, F., Carracedo, G., Otero, A., Concheiro, A., Alvarez-Lorenzo, C., 2022. Pluronic(R)/casein micelles for ophthalmic delivery of resveratrol: In vitro, ex vivo, and in vivo tests. Int. J. Pharm. 628 (122281) https://doi.org/10.1016/j.ijpharm.2022.122281.
Wang, Y., Ding, Y., Zhao, J., Wang, C., Gao, M., Chi, X., Zhang, B., Ma, X., Li, L., 2019. Dihydroartemisinin and doxorubicin co-loaded Soluplus((R))-TPGS mixed micelles: formulation characterization, cellular uptake, and pharmacodynamic studies. Pharm. Dev. Technol., 24(9), 1125-1132, doi: 10.1080/10837450.2019.1641726.
Wang, Y., Ding, Y., Xu, Y., Wang, C., Ding, Y., Gao, M., Ma, C., Ma, X., Li, L., 2020. Mixed micelles of TPGS and Soluplus((R)) for co-delivery of paclitaxel and fenretinide: in vitro and in vivo anticancer study. Pharm. Dev. Technol., 25(7), 865-873, doi: 10.1080/10837450.2020.1753770.
Wang, Y., Fan, W., Dai, X., Katragadda, U., McKinley, D., Teng, Q., Tan, C., 2014. Enhanced tumor delivery of gemcitabine via PEG-DSPE/TPGS mixed micelles. Mol. Pharm. 11 (4), 1140–1150. https://doi.org/10.1021/mp4005904.
Wang, Y., van Steenbergen, M.J., Beztsinna, N., Shi, Y., Lammers, T., van Nostrum, C.F., Hennink, W.E., 2020a. Biotin-decorated all-HPMA polymeric micelles for paclitaxel delivery. J. Control. Release 328 (970–984). https://doi.org/10.1016/j.jconrel.2020.09.013.
Wang, J., Zhang, X., Cen, Y., Lin, X., Wu, Q., 2016. Antitumor gemcitabine conjugated micelles from amphiphilic comb-like random copolymers. Colloids Surf. B Biointerfaces 146 (707–15). https://doi.org/10.1016/j.colsurfb.2016.07.027.
Wang, W., Zhong, Z., Huang, Z., Fu, F., Wang, W., Wu, L., Huang, Y., Wu, C., Pan, X., 2022. Two different protein corona formation modes on Soluplus(R) nanomicelles. Colloids Surf. B Biointerfaces 218 (112744). https://doi.org/10.1016/j.colsurfb.2022.112744.
Wilhelm, S., Tavares, A.J., Dai, Q., Ohta, S., Audet, J., Dvorak, H.F., Chan, W.C.W., 2016. Analysis of nanoparticle delivery to tumours. Nat. Rev. Mat. 1 (5), 16014. https://doi.org/10.1038/natrevmats.2016.14.
Wu, Y., Lin, J.Y., Zhou, Y.D., Liu, H.J., Lu, S.X., Zhang, X.K., Guan, Y.Y., Nagle, D.G., Zhang, W.D., Chen, H.Z., Luan, X., 2024. Oncolytic peptide-nanoplatform drives oncoimmune response and reverses adenosine-induced immunosuppressive tumor microenvironment. Adv. Healthc. Mater. https://doi.org/10.1002/adhm.202303445.
Wu, Z., Liu, C., Zhang, Z., Zheng, R., Zheng, Y., 2020b. Amidase as a versatile tool in amide-bond cleavage: From molecular features to biotechnological applications. Biotechnol. Adv. 43 (107574) https://doi.org/10.1016/j.biotechadv.2020.107574.
Wu, L., Zhang, F., Chen, X., Wan, J., Wang, Y., Li, T., Wang, H., 2020a. Self-Assembled gemcitabine prodrug nanoparticles show enhanced efficacy against patient-derived pancreatic ductal adenocarcinoma. ACS Appl. Mater. Interfaces 12 (3), 3327–3340. https://doi.org/10.1021/acsami.9b16209.
Xu, Y., Meng, H., Du, F., Lu, W., Liu, S., Huang, J., Yu, J., 2015a. Preparation of intravenous injection nanoformulation of VESylated gemcitabine by co-assembly with TPGS and its anti-tumor activity in pancreatic tumor-bearing mice. Int. J. Pharm. 495 (2), 792–797. https://doi.org/10.1016/j.ijpharm.2015.09.030.
Xu, Y., Geng, J., An, P., Xu, Y., Huang, J., Lu, W., Liu, S., Yu, J., 2015b. Cathepsin B-sensitive cholesteryl hemisuccinate–gemcitabine prodrug nanoparticles: enhanced cellular uptake and intracellular drug controlled release. RSC Adv. 5 (9), 6985–6992. https://doi.org/10.1039/C4RA13870H.
Zeng, Y.C., Li, S., Liu, C., Gong, T., Sun, X., Fu, Y., Zhang, Z.R., 2017. Soluplus micelles for improving the oral bioavailability of scopoletin and their hypouricemic effect in vivo. Acta Pharmacol. Sin. 38 (3), 424–433. https://doi.org/10.1038/aps.2016.126.
Zhang, H., He, Z., Fu, C., Pan, P., Zhu, Y., Xu, M., Deng, S., Ying, G., Shen, Y., 2022. Dissociation of polymeric micelle under hemodynamic shearing. Nano Today 45 (101517). https://doi.org/10.1016/j.nantod.2022.101517.
Zhang, Y., Kang, X., Li, J., Song, J., Li, X., Li, W., Qi, J., 2024. Inflammation-responsive nanoagents for activatable photoacoustic molecular imaging and tandem therapies in rheumatoid arthritis. ACS Nano 18 (3), 2231–2249. https://doi.org/10.1021/acsnano.3c09870.
Zhao, J., Xu, Y., Wang, C., Ding, Y., Chen, M., Wang, Y., Peng, J., Li, L., Lv, L., 2017. Soluplus/TPGS mixed micelles for dioscin delivery in cancer therapy. Drug Dev. Ind. Pharm., 43(7), 1197-1204, doi: 10.1080/03639045.2017.1304956.
Zhou, Y., Wang, C., Liu, W., Yang, M., Xu, B., Chen, Y., 2022. Fast in vitro release and in vivo absorption of an anti-schizophrenic drug paliperidone from its Soluplus/TPGS mixed micelles. Pharmaceutics 14 (5), 889. https://doi.org/10.3390/pharmaceutics14050889.
Zhou, M., Wang, Y., Xia, Y., Li, Y., Bao, J., Zhang, Y., Cheng, J., Shi, Y., 2024. MRI-guided cell membrane-camouflaged bimetallic coordination nanoplatform for combined tumor phototherapy. Materials Today Bio 26 (101019). https://doi.org/10.1016/j.mtbio.2024.101019.
Zou, D., Wu, Z., Yi, X., Hui, Y., Yang, G., Liu, Y., Tengjisi, H., Wang, A., Brooks, H., Wang, X., Liu, Z.P., Xu, M.S., Roberts, H.G., Zhao, C.X., 2023. Nanoparticle elasticity regulates the formation of cell membrane-coated nanoparticles and their nano-bio interactions. PNAS 120 (1). https://doi.org/10.1073/pnas.2214757120.